



# Improved branching-fraction measurements of $B_{(s)}^0 \rightarrow K_S^0 h^+ h'^-$ decays and first observation of $B_s^0 \rightarrow K_S^0 K^+ K^-$

LHCb collaboration<sup>†</sup>

This paper is dedicated to the memory of our friend and colleague  
Roger Barlow.

## Abstract

This paper presents a study of the charmless three-body decays  $B_{(s)}^0 \rightarrow K_S^0 h^+ h'^-$  (where  $h^{(\prime)} = \pi, K$ ), using a sample of  $pp$  collision data collected by the LHCb experiment, corresponding to an integrated luminosity of  $9 \text{ fb}^{-1}$ . The decay  $B_s^0 \rightarrow K_S^0 K^+ K^-$  is observed for the first time, and the following ratios of branching fractions are measured:

$$\begin{aligned} \frac{\mathcal{B}(B^0 \rightarrow K_S^0 K^+ K^-)}{\mathcal{B}(B^0 \rightarrow K_S^0 \pi^+ \pi^-)} &= 0.578 \pm 0.007 \pm 0.017, \\ \frac{\mathcal{B}(B^0 \rightarrow K_S^0 K^\pm \pi^\mp)}{\mathcal{B}(B^0 \rightarrow K_S^0 \pi^+ \pi^-)} &= 0.1363 \pm 0.0035 \pm 0.0051, \\ \frac{\mathcal{B}(B_s^0 \rightarrow K_S^0 \pi^+ \pi^-)}{\mathcal{B}(B^0 \rightarrow K_S^0 \pi^+ \pi^-)} &= 0.269 \pm 0.011 \pm 0.015 \pm 0.008, \\ \frac{\mathcal{B}(B_s^0 \rightarrow K_S^0 K^+ K^-)}{\mathcal{B}(B^0 \rightarrow K_S^0 \pi^+ \pi^-)} &= 0.0303 \pm 0.0041 \pm 0.0025 \pm 0.0009, \\ \frac{\mathcal{B}(B_s^0 \rightarrow K_S^0 K^\pm \pi^\mp)}{\mathcal{B}(B^0 \rightarrow K_S^0 \pi^+ \pi^-)} &= 1.818 \pm 0.021 \pm 0.031 \pm 0.056, \end{aligned}$$

where the uncertainties are statistical, systematic, and due to knowledge of the ratio of hadronisation fractions of the  $B_s^0$  and  $B^0$  mesons, respectively.

Submitted to JHEP

© 2026 CERN for the benefit of the LHCb collaboration. [CC BY 4.0 licence](https://creativecommons.org/licenses/by/4.0/).

<sup>†</sup>Authors are listed at the end of this paper.



# 1 Introduction

The charmless three-body decay processes of neutral  $B$  mesons, of the type  $B_{(s)}^0 \rightarrow K_S^0 h^+ h'^-$  ( $h^{(\prime)} = \pi, K$ ),<sup>1</sup> receive contributions from several Feynman-diagram topologies. In the Standard Model (SM), the decays  $B^0 \rightarrow K_S^0 \pi^+ \pi^-$  and  $B^0 \rightarrow K_S^0 K^+ K^-$  are particularly dominated by  $b \rightarrow q \bar{q} s$  ( $q = u, d, s$ ) loop transitions. New particles and interactions, foreseen in various SM extensions, may alter the amplitudes responsible for the decay process [1–3]. Thus, measuring the branching fractions and  $CP$ -violating asymmetries of these modes and comparing them with theoretical predictions is of great interest. As in other multibody hadronic decay modes of  $B$  hadrons, accurate theoretical predictions of branching fractions are challenging due to the presence of multiple interfering amplitudes. Precision measurements of branching fractions are therefore important inputs for further refining different theoretical approaches such as QCD factorisation or perturbative QCD [4–9], enabling better predictions of branching fractions and of  $CP$  asymmetries, both for the modes considered in this paper and for other charmless decay modes. These measurements also offer a means to evaluate the degree of isospin, U-spin, and SU(3) flavour-symmetry breaking, as illustrated, for example, in Ref. [10].

Studies of the decays of  $B^0$  mesons to  $K_S^0 \pi^+ \pi^-$ ,  $K_S^0 K^\pm \pi^\mp$ , and  $K_S^0 K^+ K^-$  final states were performed by the first-generation  $B$ -factory experiments, BaBar and Belle [11–15]. The first study of  $B_{(s)}^0 \rightarrow K_S^0 h^+ h'^-$  branching fractions performed by the LHCb collaboration, using the data sample recorded in 2011 corresponding to an integrated luminosity of  $1 \text{ fb}^{-1}$  [16], reported the first observation of  $B_s^0 \rightarrow K_S^0 \pi^+ \pi^-$  and  $B_s^0 \rightarrow K_S^0 K^\pm \pi^\mp$  decays, but found no evidence for the  $B_s^0 \rightarrow K_S^0 K^+ K^-$  decay. This study was subsequently updated with the full 2011–2012 data sample, corresponding to an integrated luminosity of  $3.0 \text{ fb}^{-1}$  [17]; once again, no conclusive evidence for the decay  $B_s^0 \rightarrow K_S^0 K^+ K^-$  was found, with the significance of the corresponding signal found to be 2.5 standard deviations. The search reported here, using a much larger data sample, is therefore strongly motivated.

The selection criteria and mass fit procedures developed in this analysis for branching-fraction measurements may be reused in subsequent amplitude analyses, which provide access to more observables enabling detailed understanding of the decay dynamics. In such analyses, the contributing intermediate resonances can be disentangled, allowing the branching fractions and  $CP$ -violation parameters of the intermediate decay modes to be determined. The measurement of such  $CP$ -violation observables in  $B_{(s)}^0 \rightarrow K_S^0 h^+ h'^-$  decays is of significant theoretical interest. In particular, the mixing-induced  $CP$  asymmetries in the decays dominated by loop transitions, such as  $B^0 \rightarrow \phi K_S^0$ , are predicted by the Cabibbo–Kobayashi–Maskawa (CKM) paradigm [18, 19] to differ only slightly from those of  $b \rightarrow c \bar{c} s$  transitions, such as  $B^0 \rightarrow J/\psi K_S^0$ . Within the SM, any deviations are expected to be small or may be controlled through flavour symmetries [20–22], whereas new particles and interactions could introduce additional weak phases, potentially leading to significantly larger deviations [1–3]. The mixing-induced  $CP$ -violating phase can be determined through a flavour-tagged, time-dependent amplitude analysis within the phase space of these three-body decay processes [13, 15, 23, 24]. The current experimental uncertainties [25, 26] remain substantially larger than the expected deviations, both within the SM and in scenarios extending beyond it, thereby motivating more precise measurements of these observables. Similarly, the mixing-induced  $CP$ -violating phase in the  $B_s^0$  system could be measured

---

<sup>1</sup>Unless stated otherwise, charge-conjugate modes are implicitly included throughout this article.

through  $b \rightarrow q\bar{q}s$  processes such as  $B_s^0 \rightarrow K_S^0 K^\pm \pi^\mp$  decays [27]. The CKM angle  $\gamma$  can also be determined by combining information obtained from several  $B \rightarrow Khh'$  decays, including the branching fractions of these modes [28–30]. Experimental results from the BaBar collaboration [31, 32] demonstrate the feasibility of this measurement, albeit with large statistical uncertainties. Another method was suggested in Refs. [33–35] and applied to amplitude models previously measured by BaBar [36], yielding several possible values of  $\gamma$ . The decay  $B_s^0 \rightarrow K_S^0 \pi^+ \pi^-$  is dominated by tree-level processes, and thus offers a potential theoretically cleaner determination of the angle  $\gamma$  [37].

In this paper, decays of  $B^0$  and  $B_s^0$  mesons to the charmless three-body final states  $K_S^0 \pi^+ \pi^-$ ,  $K_S^0 K^\pm \pi^\mp$ , and  $K_S^0 K^+ K^-$  are studied with the  $pp$  collision data recorded by the LHCb detector, corresponding to an integrated luminosity of  $1.0 \text{ fb}^{-1}$  at a centre-of-mass energy of  $\sqrt{s} = 7 \text{ TeV}$  in 2011,  $2.0 \text{ fb}^{-1}$  at  $\sqrt{s} = 8 \text{ TeV}$  in 2012, and  $6 \text{ fb}^{-1}$  at  $\sqrt{s} = 13 \text{ TeV}$  from 2015 to 2018. The integrated luminosity is approximately three times larger than that used in Ref. [17], which this paper supersedes. Furthermore, the production cross-section of  $B^0$  and  $B_s^0$  mesons increases with the centre-of-mass energy [38]. The time-integrated,  $CP$ -averaged branching fractions are measured relative to the  $B^0 \rightarrow K_S^0 \pi^+ \pi^-$  decay. For  $B_s^0$  decays, this implies that the contribution arising from nonzero width difference is included [39]. Throughout this document, the notation  $\mathcal{B}(B^0 \rightarrow K_S^0 K^\pm \pi^\mp)$  refers to the sum of the branching fractions  $\mathcal{B}(B^0 \rightarrow K_S^0 K^+ \pi^-)$  and  $\mathcal{B}(B^0 \rightarrow K_S^0 K^- \pi^+)$ , and the same applies to the corresponding  $B_s^0$  decays.

## 2 Detector and simulation

The LHCb detector [40, 41] is a single-arm forward spectrometer covering the pseudorapidity range  $2 < \eta < 5$ , designed for the study of particles containing  $b$  or  $c$  quarks. The detector used to collect the data analysed in this paper includes a high-precision tracking system consisting of a silicon-strip vertex detector surrounding the  $pp$  interaction region (the VELO), a large-area silicon-strip detector located upstream of a dipole magnet with a bending power of about  $4 \text{ T m}$ , and three stations of silicon-strip detectors and straw drift tubes placed downstream of the magnet. The tracking system provides a measurement of the momentum,  $p$ , of charged particles with a relative uncertainty that varies from 0.5% at low momentum to 1.0% at  $200 \text{ GeV}/c$ . The minimum distance of a track to a primary  $pp$  collision vertex (PV), the impact parameter (IP), is measured with a resolution of  $(15 + 29/p_T) \mu\text{m}$ , where  $p_T$  is the component of the momentum transverse to the beam, in  $\text{GeV}/c$ . Different types of charged hadrons are distinguished using information from two ring-imaging Cherenkov detectors. Photons, electrons and hadrons are identified by a calorimeter system consisting of scintillating-pad and preshower detectors, an electromagnetic and a hadronic calorimeter. Muons are identified by a system composed of alternating layers of iron and multiwire proportional chambers.

Simulation is required to model the effects of the detector acceptance and selection requirements and to investigate backgrounds from other  $b$ -hadron decays. In the simulation,  $pp$  collisions are generated using PYTHIA [42] with a specific LHCb configuration [43]. Decays of unstable particles are described by EVTGEN [44], in which final-state radiation is generated using PHOTOS [45]. The interaction of the generated particles with the detector, and its response, are implemented using the GEANT4 toolkit [46] as described

in Ref. [47].

To account for possible mismodelling of the detector response in simulation, in particular that of the particle identification (PID) systems, dedicated data and simulated calibration samples are used to correct the values of the corresponding variables for each candidate reconstructed in the simulated signal samples. The PID corrections are based on matching the cumulative distribution function (CDF) of the variable in question between the data and simulation calibration samples [48]. The variation of the PID response with the kinematics of the track and the occupancy of the detector is accounted for using a kernel density estimation in the four dimensions: PID variable CDF,  $p_T$  and  $\eta$  of the track, and the track multiplicity of the event [49].

### 3 Trigger and event selection

The online event selection is performed by a trigger [50], which consists of a hardware stage, based on information from the calorimeter and muon systems, followed by a software stage, which applies a full event reconstruction. At the hardware trigger level, events are required to have a muon with high  $p_T$  or a hadron, photon or electron with high transverse energy in the calorimeters. For the decay modes considered, all of these triggers can be caused by activity in the event not associated with the signal candidate and, for the hadron triggers, they can also be caused by the signal candidate itself. The software trigger requires a two-, three- or four-track secondary vertex with a significant displacement from all primary  $pp$  interaction vertices. At least one charged particle must have high transverse momentum and be inconsistent with originating from any reconstructed PV. A multivariate algorithm [51, 52] is used for the identification of secondary vertices consistent with the decay of a  $b$  hadron. It is required that the software trigger decision must have been caused entirely by tracks from the decay of the signal  $B$  candidate.

To suppress background, events satisfying the trigger requirements are filtered in two subsequent stages: a set of loose preselection requirements, followed by an optimised multivariate selection. A potential source of systematic uncertainty is the accuracy of modelling the variation of the selection efficiency over the phase space of the  $B$  decay. To mitigate this, the selection is designed to minimise efficiency variations by imposing only loose requirements on properties (such as the momenta) of the individual  $B$ -meson decay products. Instead, extensive use is made of topological features such as the flight distance of the  $B$  candidate. The calculated values of these features depend on the assumption that the  $B$  candidate (or its decay products) have originated from a particular PV. To remove ambiguity, it is therefore necessary to associate each candidate with a single PV, that from which it is most consistent with having originated. The metric for defining the consistency is the  $\chi_{\text{IP}}^2$  quantity, which is the difference in vertex-fit  $\chi^2$  of the given PV reconstructed with and without the candidate in question. In events that contain more than one PV, each candidate is associated with the PV with which it forms the smallest  $\chi_{\text{IP}}^2$  value.

Candidate  $K_S^0 \rightarrow \pi^+ \pi^-$  decays are reconstructed in two different categories: the first involving  $K_S^0$  mesons that decay early enough for the resulting pions to be reconstructed in the VELO; and the second contains those  $K_S^0$  mesons that decay further downstream, such that track segments of the pions cannot be formed in the VELO. These  $K_S^0$  reconstruction categories are referred to as *long* (LL) and *downstream* (DD), respectively. The long

category has better mass, momentum and vertex resolution than the downstream category. There are, however, approximately twice as many  $K_S^0$  candidates reconstructed as DD than as LL, due to the lifetime of the  $K_S^0$  meson and the geometry of the detector. In the following,  $B$  candidates whose decay products include either a long or downstream  $K_S^0$  candidate are referred to using the corresponding category names. During the 2012 data taking, a significant improvement of the trigger efficiency for downstream  $K_S^0$  candidates was obtained following an update of the software trigger algorithms. To take this into account, the 2012 data sample is subdivided into the 2012a and 2012b data-taking periods.

The  $K_S^0$  candidates are formed by combining two oppositely charged pions, both of which are required to have momentum  $p > 2 \text{ GeV}/c$  and have  $\chi_{\text{IP}}^2$  with respect to their associated PV greater than 9 (4) for long (downstream) candidates. The vertex of the  $K_S^0$  candidate is determined and the resulting mass must be within  $\pm 20 \text{ MeV}/c^2$  ( $\pm 30 \text{ MeV}/c^2$ ) of the known  $K_S^0$  mass [26] for long (downstream) candidates. To discriminate against tracks originating from the PV, the  $K_S^0$  vertex is required to be significantly displaced from its associated PV, as quantified by  $\chi_{\text{VS}}^2$ , the difference in vertex-fit  $\chi^2$  when the secondary vertex is constrained to coincide with the primary vertex. In addition, downstream  $K_S^0$  candidates are required to have a momentum  $p > 6 \text{ GeV}/c$ .

The  $B$  candidates are formed by combining a  $K_S^0$  candidate and two oppositely charged particles,  $h^+h^-$ , initially assuming the pion-mass hypothesis. The momenta of both charged particles are required to be in the range  $3 < p < 100 \text{ GeV}/c$  to ensure good pion-kaon discrimination. Both charged particles should also be inconsistent with being muons based on information from the muon system. The scalar sum of the transverse momenta of the  $K_S^0$ ,  $h^+$ , and  $h^-$  candidates must be greater than  $3.0 \text{ GeV}/c$  ( $4.2 \text{ GeV}/c$ ), for long (downstream) candidates, and at least two of the three decay products must have  $p_{\text{T}} > 0.8 \text{ GeV}/c$ . The  $B$  candidates must have  $p_{\text{T}} > 1.5 \text{ GeV}/c$  and mass within the range  $4000 < m_{K_S^0\pi^+\pi^-} < 6200 \text{ MeV}/c^2$ . The fitted  $B$ -candidate decay vertex should be significantly separated from any PV, and isolated from other tracks, as quantified by the change in vertex-fit chi-square,  $\chi_{\text{vtx}}^2$ , when adding any other track in the event. The  $B$  candidates should also be consistent with originating from a PV, quantified by requiring, for long (downstream) candidates, both that  $\chi_{\text{IP}}^2 < 8$  (6) and that the cosine of the angle  $\theta_{\text{DIR}}$  between the reconstructed momentum vector of the  $B$  candidate and the vector between the associated PV and the decay vertex be greater than 0.9999 (0.999). Finally, the decay vertex of the  $K_S^0$  candidate is required to be at least 30 mm downstream, along the beam direction, from that of the  $B$  candidate. In conjunction with the  $K_S^0$  mass requirement, this suppresses direct four-body decays  $B_{(s)}^0 \rightarrow h^+h^-\pi^+\pi^-$ , as well as misreconstructed  $B_{(s)}^0 \rightarrow K_S^0h^+h^-$  decays in which a pion produced in the  $K_S^0$  decay is exchanged with the  $h$  or  $h'$  track of the same charge.

The next stage of the selection uses dedicated multivariate discriminants trained using the XGBOOST implementation [53] of a boosted decision tree (BDT) algorithm [54]. Two different types of classifiers are trained, each designed to suppress a particular background contribution. The first is designed to suppress the combinatorial background and mainly uses information on the decay topology. Since the different signal channels have almost identical topologies, the same BDT is used for all channels. In contrast, the second classifier, referred to as the PID BDT in the following, is designed to suppress background from so-called cross-feed backgrounds, where a signal decay from one signal channel is misidentified as being from another signal channel, *e.g.* a  $B_s^0 \rightarrow K_S^0K^\pm\pi^\mp$  decay where the final-state kaon is misidentified as a pion and so is reconstructed as a candidate in the

$K_S^0\pi^+\pi^-$  spectrum. Accordingly, this latter classifier is trained using information from the particle-identification systems and separate classifiers are trained for each of the signal final states.

The features used in the topological BDT training are: the  $p_T$ ,  $\eta$ ,  $\chi_{IP}^2$ ,  $\chi_{VS}^2$ ,  $\cos\theta_{DIR}$  and  $\chi_{vtx}^2$  values of the  $B$  candidate; the smallest change in the  $B$ -candidate  $\chi_{vtx}^2$  value when adding another track from the event; the sum of the  $\chi_{IP}^2$  values of the  $h^+$  and  $h^-$  candidates and, in the case of the long category, additionally that of the  $K_S^0$  candidate; and the  $\chi_{VS}^2$  of the  $K_S^0$  candidate for the long category only. Additional variables included are four asymmetries of the form

$$X^{\text{asym}} \equiv \frac{X^P - X^{\text{cone}}}{X^P + X^{\text{cone}}}, \quad (1)$$

where  $X^P$  is the quantity  $X$  ( $p$  or  $p_T$ ) for particle  $P$  ( $B$  or  $K_S^0$ ) and  $X^{\text{cone}}$  is the same quantity determined from a vector sum of the momenta of all charged tracks inside a cone around the direction of particle  $P$ , of radius  $R \equiv \sqrt{\delta\eta^2 + \delta\phi^2} = 1.5$ . Here  $\delta\eta$  and  $\delta\phi$  are the difference in pseudorapidity and azimuthal angle (in radians) around the beam direction, between the momentum vector of the track under consideration and that of particle  $P$ . Finally, four differences of the form

$$Y^{\text{diff}} \equiv Y^P - Y^{\text{cone}}, \quad (2)$$

where the quantity  $Y$  is either  $\eta$  or  $\phi$ , are also included in the BDT. The signal and background training samples are, respectively, simulated  $B^0 \rightarrow K_S^0\pi^+\pi^-$  decays and data from the upper mass sideband,  $5425 < m_{K_S^0\pi^+\pi^-} < 6200 \text{ MeV}/c^2$ . Contributions from  $\Lambda_b^0 \rightarrow \Lambda_c^+h^-$ ,  $\Lambda_c^+ \rightarrow K_S^0p$  decays are removed from the training samples taken from data, using mass vetoes.

The features used to train the PID BDT are the outputs of multivariate classifiers applied to the  $h^+$  and  $h^-$  candidates, each designed to identify kaons, pions, and protons using information from the particle-identification and tracking detectors. The PID BDT for a given final state is trained using simulation, where the signal training sample consists of decays of the channel in question, while the background training sample contains different  $B_{(s)}^0 \rightarrow K_S^0h^+h^-$  decay modes. For both signal and background training samples, the candidates are reconstructed under the mass hypothesis of the final state being considered, meaning that in the background sample one of the final-state hadrons has been assigned the wrong identity.

The selection requirements placed on the output of the two BDTs are simultaneously optimised. The optimisation is performed independently for each data-taking year, with 2012 subdivided as mentioned above, and for each  $K_S^0$  reconstruction type. Moreover, as each final state contains both  $B^0$  and  $B_s^0$  signals, one of which is favoured and the other suppressed, a separate optimisation is performed for each of these decay modes, resulting in a tighter and looser selection for each final state. For all signal decay modes that have previously been observed, the following figure of merit is used

$$\mathcal{Q}_1 \equiv \frac{N_{\text{sig}}}{\sqrt{N_{\text{sig}} + N_{\text{bg}}}}, \quad (3)$$

where  $N_{\text{sig}}$  ( $N_{\text{bg}}$ ) represents the number of expected signal (combinatorial background) candidates that are retained by a given selection and fall within the signal region. The

signal region is defined as a mass window of  $\pm 2.5$  times the estimated signal resolution around the known  $B^0$  or  $B_s^0$  mass [26], as appropriate. The value of  $N_{\text{sig}}$  is estimated based on the known branching fractions [26] and the signal efficiency ( $\varepsilon_{\text{sig}}$ ) determined from simulation. Due to the simultaneous optimisation of the two BDTs, the calculation of  $N_{\text{bg}}$  must include both combinatorial and cross-feed background sources. The expected number of cross-feed candidates is calculated similarly to  $N_{\text{sig}}$ , while the number of expected combinatorial candidates is determined by fitting the mass distribution above the signal region ( $5550 < m_{K_S^0 h^+ h'^-} < 6200 \text{ MeV}/c^2$ ) and extrapolating into the signal region. The  $B_s^0 \rightarrow K_S^0 K^+ K^-$  mode is yet to be observed and so an alternative figure of merit is used that does not require knowledge of the signal branching fraction [55],

$$\mathcal{Q}_2 \equiv \frac{\varepsilon_{\text{sig}}}{\frac{5}{2} + \sqrt{N_{\text{bg}}}}, \quad (4)$$

where the value of  $N_{\text{bg}}$  is estimated in the same way as described for  $\mathcal{Q}_1$ .

A final category of background that must be considered consists of fully reconstructed  $b$ -hadron decays into a  $K_S^0 h^+ h'^-$  final state that proceed via an intermediate charm or charmonium state, *e.g.* two-body  $Dh$ ,  $\Lambda_c^+ h$  or  $(c\bar{c})K_S^0$  combinations, where  $(c\bar{c})$  indicates a charmonium resonance. Such decays often satisfy the selection criteria with reasonably high efficiency and may result in a very similar  $B$ -candidate mass distribution as the signal candidates. Therefore, the following decays are explicitly reconstructed under the relevant particle mass hypotheses and vetoed in all the spectra:  $D^0 \rightarrow K^- \pi^+$ ,  $D^+ \rightarrow K_S^0 K^+$ ,  $D^+ \rightarrow K_S^0 \pi^+$ ,  $D_s^+ \rightarrow K_S^0 K^+$ ,  $D_s^+ \rightarrow K_S^0 \pi^+$ ,  $\Lambda_c^+ \rightarrow p K_S^0$ ,  $J/\psi \rightarrow \pi^+ \pi^-$ ,  $J/\psi \rightarrow K^+ K^-$ ,  $\chi_{c0} \rightarrow \pi^+ \pi^-$ , and  $\chi_{c0} \rightarrow K^+ K^-$ . The vetoed mass region for each reconstructed charm (charmonium) state is a window of  $\pm 30$  ( $\pm 48$ )  $\text{MeV}/c^2$  around the known mass of that state [26]. This range reflects the typical mass resolution obtained at LHCb. Similarly, backgrounds from  $\Lambda \rightarrow p \pi^-$  decays being reconstructed as  $K_S^0 \rightarrow \pi^+ \pi^-$  are suppressed by applying a mass veto window of  $\pm 6.8 \text{ MeV}/c^2$  around the known  $\Lambda$  mass [26] when applying the  $p \pi^-$  or  $\pi^+ \bar{p}$  mass hypothesis to the  $K_S^0$ -candidate decay products.

## 4 Fit model

The data are divided into seven statistically independent subsamples, separated by data-taking period (2011, 2012a, 2012b, 2015, 2016, 2017, 2018). The selected  $B$  candidates form eight mass spectra: four final states ( $K_S^0 \pi^+ \pi^-$ ,  $K_S^0 K^+ \pi^-$ ,  $K_S^0 \pi^+ K^-$ ,  $K_S^0 K^+ K^-$ ) multiplied by two  $K_S^0$  reconstruction types (LL, DD). For each subsample, simultaneous unbinned maximum-likelihood fits to the eight mass spectra in the range 5100–5750  $\text{MeV}/c^2$  are used to determine the signal yields. In general, each final state will contain two signal peaks,  $B^0$  and  $B_s^0$ , and, as discussed above, the optimum working point in the selection is significantly different between the two peaks. To minimise the expected statistical uncertainties on the ratios of branching fractions, the fit procedure described below is performed twice for each subsample: once with the tighter selections, to be used to measure the branching fractions of the  $B^0 \rightarrow K_S^0 K^\pm \pi^\mp$ ,  $B_s^0 \rightarrow K_S^0 \pi^+ \pi^-$ , and  $B_s^0 \rightarrow K_S^0 K^+ K^-$  decays relative to that of the  $B^0 \rightarrow K_S^0 \pi^+ \pi^-$  decay; and once with the looser selections, to be used to measure the branching fractions of the  $B^0 \rightarrow K_S^0 K^+ K^-$  and  $B_s^0 \rightarrow K_S^0 K^\pm \pi^\mp$  decays relative to that of the  $B^0 \rightarrow K_S^0 \pi^+ \pi^-$  decay.

Several different components contribute to each mass spectrum. Those considered in the baseline fit model are the two signal peaks arising from correctly reconstructed  $B^0$  and  $B_s^0$  signal decays, cross-feed structures due to other  $B_{(s)}^0 \rightarrow K_S^0 h^+ h'^-$  decays in which one or both charged hadrons is misidentified, partially reconstructed decays of a  $b$  hadron to a final state of the form  $K_S^0 h^+ h'^- X$  where the system  $X$  is not reconstructed, and combinatorial background.

Each signal peak is modelled as the sum of two Crystal Ball functions [56], which share common peak position ( $\mu$ ) and width ( $\sigma$ ) parameters, but whose power-law tails are on opposite sides of the peak and have separate parameters ( $n_L, n_R, \alpha_L, \alpha_R$ ). An additional parameter ( $f_L$ ) determines the fraction of candidates in the left-tailed Crystal Ball function, for a total of seven shape parameters. A simultaneous fit to the eight mass spectra in simulated signal events of the subsample under consideration is used to determine the lineshape parameters, with certain parameters (or ratios of parameters) shared between mass spectra and between the  $B^0$  and  $B_s^0$  peaks; see Appendix B for details. In particular, the peak position parameters  $\mu(B^0)$  and  $\mu(B_s^0)$  are common across all spectra, and the width parameters  $\sigma$  are defined relative to one reference peak, corresponding to the  $B^0 \rightarrow K_S^0 \pi^+ \pi^-$  decay with downstream  $K_S^0$  reconstruction. When fitting to a subsample of data, only two of the signal shape parameters are free to vary, with all others being derived from those two or fully fixed from the fit to simulated data. The two free shape parameters are the  $B^0$  peak position parameter, with the  $B_s^0$  peak position derived according to  $\mu(B_s^0) = \mu(B^0) + \Delta m$ , where  $\Delta m = 87.26 \text{ MeV}/c^2$  is the known difference in mass between the two states [26]; and the peak width parameter  $\sigma(B^0 \rightarrow K_S^0 \pi^+ \pi^-; \text{DD})$ , with all other width parameters derived from it according to the ratios seen in the fit to simulation. It has been determined that the ratio of the widths in the downstream and long  $K_S^0$  reconstruction types of the  $B^0 \rightarrow K_S^0 \pi^+ \pi^-$  channel is well reproduced in the simulation. All signal yields are free to vary in the fit to data.

Cross-feed components occur due to hadron misidentification of the  $h^+$  or  $h'^-$  mesons, such that events from one of the eight signal decay modes appear in a different mass spectrum, *e.g.*  $B^0 \rightarrow K_S^0 \pi^+ \pi^-$  decays may appear in the  $K_S^0 K^+ \pi^-$  spectrum if the  $\pi^+$  is misidentified as a  $K^+$ . The probability for a misidentified decay to pass the selection is determined with simulation, corrected for known data-simulation differences, in the same way as the efficiency for a correctly identified decay to pass the selection, as described in Sec. 6. Cross-feed components are modelled with the same functional form as the signal. For each combination of a true decay and reconstructed final state, the shape parameters are determined from a fit to simulated signal events of the true decay that pass the selection for the reconstructed final state. This fit is performed simultaneously to all data-taking periods and to both  $K_S^0$  reconstruction types, and with the final states  $K_S^0 K^+ \pi^-$  and  $K_S^0 \pi^+ K^-$  combined. Double misidentification (*e.g.*  $B^0 \rightarrow K_S^0 \pi^+ \pi^-$  decays identified as  $K_S^0 K^+ K^-$ ) is found to be negligible, as is cross-feed from the suppressed decays  $B_s^0 \rightarrow K_S^0 \pi^+ \pi^-$  and  $B_s^0 \rightarrow K_S^0 K^+ K^-$ . This leaves two cross-feed structures in each final state:  $B^0 \rightarrow K_S^0 K^\pm \pi^\mp$  and  $B_s^0 \rightarrow K_S^0 K^\pm \pi^\mp$  in  $K_S^0 \pi^+ \pi^-$ ;  $B^0 \rightarrow K_S^0 \pi^+ \pi^-$  and  $B^0 \rightarrow K_S^0 K^+ K^-$  in  $K_S^0 K^\pm \pi^\mp$ ; and  $B^0 \rightarrow K_S^0 K^\pm \pi^\mp$  and  $B_s^0 \rightarrow K_S^0 K^\pm \pi^\mp$  in  $K_S^0 K^+ K^-$ . When fitting to a subsample of data, the shape of each cross-feed component is fixed from the fit to simulated data. Since the misidentification probabilities are known from simulation, the yield of each misidentified, cross-feed contribution may be constrained from the yield of the corresponding correctly identified signal component with the same  $K_S^0$  reconstruction. For each final state, this is implemented by constraining the ratio of the yields of the two cross-feed structures; this

leaves one free cross-feed yield-normalisation parameter per final state. In addition, when applying the tighter selection, a second constraint is added, such that the cross-feed yields are fully determined by the correctly identified signal yields and the misidentification probabilities.

A range of different physical processes contribute to partially reconstructed components; in each case, one or more final-state particles from the true decay are omitted in the reconstruction (*e.g.*  $B^0 \rightarrow K^{*0}\pi^+\pi^-$ ,  $K^{*0} \rightarrow K_S^0\pi^0$  with the  $\pi^0$  omitted). Because part of the four-momentum is missing in such decays, the lineshape is, in general, displaced to lower mass. Since the fit range starts at 5100 MeV/ $c^2$ , a complete description of all partially reconstructed decays is not required: often, the bulk of their distribution lies below the lower fit boundary. Instead, simulated samples of a small number of decay modes are used, and in each case the lineshape is modelled as the convolution of a generalised ARGUS function [57] with a Gaussian function, using a simultaneous fit to all data-taking periods and to both  $K_S^0$  reconstruction types. For partially reconstructed charmless decays, the representative decay mode used is  $B^0 \rightarrow K^*(892)^0\rho(770)^0$ , with  $K^*(892)^0 \rightarrow K_S^0\pi^0$  and  $\rho(770)^0 \rightarrow \pi^+\pi^-$  with the  $\pi^0$  omitted, and the lineshape obtained is used for all final states and for both partially reconstructed  $B_{d/u}$  and  $B_s^0$  decays (with an offset of  $+\Delta m$  when the source is a  $B_s^0$  decay). When fitting to a subsample of data, the shape of each partially reconstructed component is fixed from the fits to simulated data. Each final state contains two charmless partially reconstructed components ( $B_{d/u}$  and  $B_s^0$ ), and their yields are free to vary in the fit to data. Other contributions are considered as systematic variations, as described in Sec. 6.1.

The combinatorial background component, arising from unrelated or uncorrelated combinations of final-state particles, is parameterised as a first-order polynomial function. When fitting to a subsample of data, the yield and slope of the combinatorial component are free to vary for each final state, except that the  $K_S^0K^+\pi^-$  and  $K_S^0\pi^+K^-$  final states share a common slope parameter.

The individual fits to the subsamples can be found in Appendix A. For illustration, the sum of all of the individual fits are shown, together with the combined dataset, in Fig. 1 for the tighter selection, and in Fig. 2 for the looser selection. The total fitted signal yields, summed across all subsamples, are given in Table 1 with statistical uncertainties only. In addition to the signal yields, the fit output is also used to compute signal weights via the *sPlot* method [58, 59]; these are used for certain data-simulation corrections as described below. The total yield of  $B_s^0 \rightarrow K_S^0K^+K^-$ , combining the long and downstream  $K_S^0$  reconstruction types, is found to be  $207 \pm 21$  with the tighter selection, for which the corresponding significance, based on the ratio of yield to statistical uncertainty, is approximately 10 standard deviations.

## 5 Determination of the efficiencies

The following expression is used to determine branching fractions of the  $B_{(s)}^0 \rightarrow K_S^0h^+h'^-$  decays relative to the normalisation mode  $B^0 \rightarrow K_S^0\pi^+\pi^-$ ,

$$\frac{\mathcal{B}(B_{(s)}^0 \rightarrow K_S^0h^+h'^-)}{\mathcal{B}(B^0 \rightarrow K_S^0\pi^+\pi^-)} = \frac{\varepsilon_{B^0 \rightarrow K_S^0\pi^+\pi^-}^{\text{sel}}}{\varepsilon_{B_{(s)}^0 \rightarrow K_S^0h^+h'^-}^{\text{sel}}} \frac{N_{B_{(s)}^0 \rightarrow K_S^0h^+h'^-}}{N_{B^0 \rightarrow K_S^0\pi^+\pi^-}} \frac{f_d}{f_{d(s)}}, \quad (5)$$

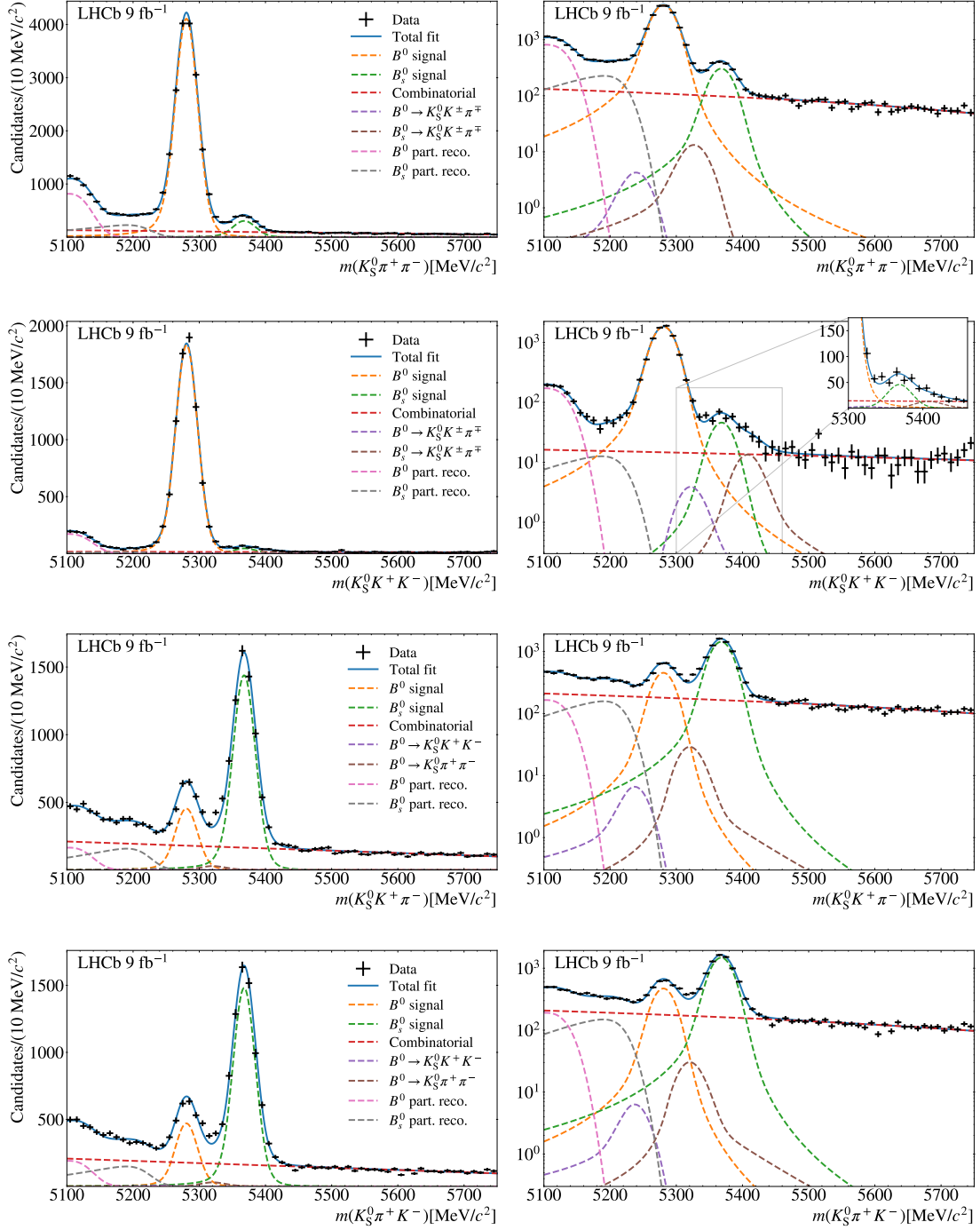


Figure 1: Mass distributions of  $K_S^0 h^+ h'^-$  candidates that pass the tighter selection, combining all running periods and both  $K_S^0$  reconstruction types. For illustration, the sum of the fits to the subsamples is also shown. From top to bottom, each row corresponds to a different final state:  $K_S^0 \pi^+ \pi^-$ ,  $K_S^0 K^+ K^-$ ,  $K_S^0 K^+ \pi^-$ ,  $K_S^0 \pi^+ K^-$ . The inset zooms into the  $B_s^0 \rightarrow K_S^0 K^+ K^-$  signal region.

where  $\varepsilon_X^{\text{sel}}$  denotes the average efficiency of the decay mode  $X$ ,  $N_X$  is the fitted signal yield, and  $f_d$  and  $f_s$  are the hadronisation fractions of a  $b$  quark into a  $B^0$  or  $B_s^0$  meson,

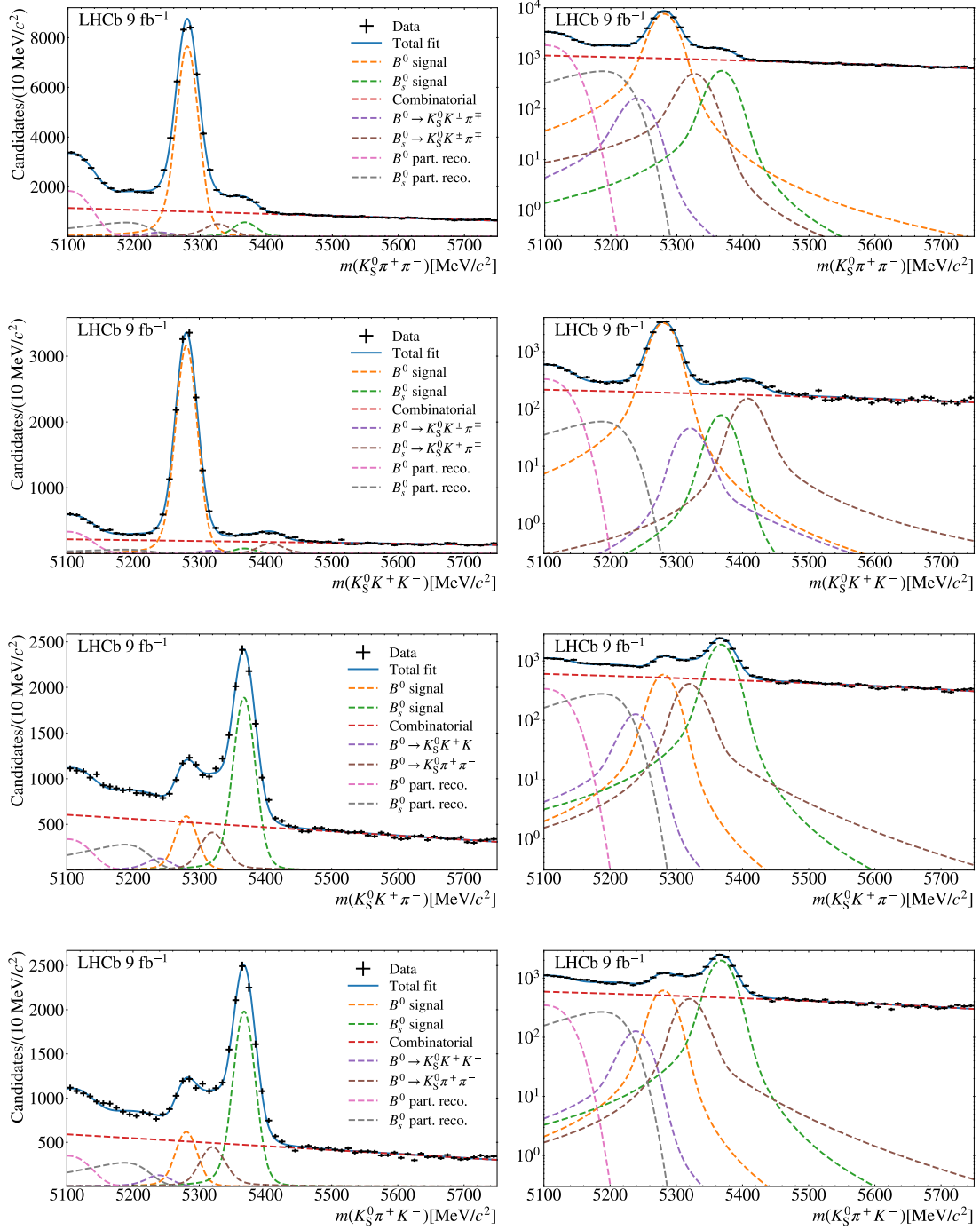


Figure 2: Mass distributions of  $K_S^0 h^+ h'^-$  candidates that pass the looser selection, combining all running periods and both  $K_S^0$  reconstruction types. For illustration, the sum of the fits to the subsamples is also shown. From top to bottom, each row corresponds to a different final state:  $K_S^0 \pi^+ \pi^-$ ,  $K_S^0 K^+ K^-$ ,  $K_S^0 K^+ \pi^-$ ,  $K_S^0 \pi^+ K^-$ .

respectively. The efficiency term includes the geometrical acceptance and the trigger, reconstruction, and selection requirements. The ratio  $f_s/f_d$  has been measured previously at the LHCb experiment using hadronic and semileptonic decays at different centre-of-

Table 1: Signal yields and the associated statistical uncertainties for each final state in data, combining results from fits to the seven data-taking periods, obtained at the two different selection working points (looser, tighter). Yields are quoted separately for the two  $K_S^0$  reconstruction types (LL, DD).

Decay	Yield (looser)	Yield (tighter)
$B^0 \rightarrow K_S^0(\text{LL})\pi^+\pi^-$	$10930 \pm 140$	$6920 \pm 90$
$B^0 \rightarrow K_S^0(\text{DD})\pi^+\pi^-$	$25040 \pm 230$	$12360 \pm 120$
$B^0 \rightarrow K_S^0(\text{LL})K^+K^-$	$4280 \pm 70$	$2700 \pm 50$
$B^0 \rightarrow K_S^0(\text{DD})K^+K^-$	$9640 \pm 120$	$5320 \pm 80$
$B^0 \rightarrow K_S^0(\text{LL})\pi^+K^-$	$830 \pm 50$	$700 \pm 40$
$B^0 \rightarrow K_S^0(\text{DD})\pi^+K^-$	$1940 \pm 90$	$1430 \pm 60$
$B^0 \rightarrow K_S^0(\text{LL})K^+\pi^-$	$720 \pm 50$	$576 \pm 35$
$B^0 \rightarrow K_S^0(\text{DD})K^+\pi^-$	$1910 \pm 90$	$1480 \pm 60$
$B_s^0 \rightarrow K_S^0(\text{LL})\pi^+\pi^-$	$820 \pm 60$	$485 \pm 34$
$B_s^0 \rightarrow K_S^0(\text{DD})\pi^+\pi^-$	$1920 \pm 110$	$980 \pm 50$
$B_s^0 \rightarrow K_S^0(\text{LL})K^+K^-$	$88 \pm 27$	$60 \pm 12$
$B_s^0 \rightarrow K_S^0(\text{DD})K^+K^-$	$270 \pm 50$	$147 \pm 17$
$B_s^0 \rightarrow K_S^0(\text{LL})\pi^+K^-$	$2750 \pm 70$	$2130 \pm 50$
$B_s^0 \rightarrow K_S^0(\text{DD})\pi^+K^-$	$6300 \pm 110$	$4690 \pm 80$
$B_s^0 \rightarrow K_S^0(\text{LL})K^+\pi^-$	$2550 \pm 70$	$1970 \pm 50$
$B_s^0 \rightarrow K_S^0(\text{DD})K^+\pi^-$	$6080 \pm 110$	$4660 \pm 80$

mass energies [60]. When calculating the branching fraction for a given data subsample, the value of  $f_s/f_d$  used is that corresponding to the centre-of-mass energy at which the subsample was recorded. The uncertainty on  $f_s/f_d$  is treated as being fully correlated across all subsamples.

Three-body hadronic decays such as  $B_{(s)}^0 \rightarrow K_S^0 h^+ h'^-$  may proceed through quasi-two-body intermediate resonances, and may also include broad amplitudes, referred to as nonresonant, that may overlap and interfere with one another. The resulting distribution of events within the phase space is characterised as a Dalitz plot [61]. In the case of charmless three-body  $b$ -meson decays, the distribution is far from uniform, typically with much higher probability density near the boundaries of the Dalitz plot (as illustrated for the decay  $B_s^0 \rightarrow K_S^0 K^\pm \pi^\mp$  in Ref. [62]). Because the trigger, reconstruction, and selection efficiencies can vary considerably across the Dalitz plot, the efficiency  $\varepsilon_X^{\text{sel}}$  is obtained by a weighted average across the phase space, with weights computed from the signal distribution. The signal distributions are determined from the data sample analysed: although for certain decay modes there are prior measurements of the Dalitz-plot distribution, these are drawn from smaller signal yields.

To simplify the description of the phase space, a transformation into a square Dalitz plot [63] is used; this has the benefit of spreading out the regions close to the kinematic boundaries where resonances are concentrated and where the efficiency varies rapidly. The square Dalitz plot is divided into bins in a  $10 \times 10$  grid. For a data-taking period  $k$ , the efficiency within bin  $j$  is denoted  $\varepsilon_{j,k}$  and is computed from simulated events, corrected

for known data-simulation differences as described below.

For each subsample  $k$  of data, the fits to the  $K_S^0 h^+ h'^-$  mass spectra described in Sec. 4 are used to generate weights,  $W_{j,k}$ , using the *sPlot* technique [59], taking the  $K_S^0 h^+ h'^-$  mass as the discriminating variable; these weights are then used to isolate the  $B^0$  and  $B_s^0$  signals in data and determine their distributions in the square Dalitz plots. Correlations between the Dalitz-plot variables and the discriminating variable are found to be sufficiently small to be neglected. While this can be done for all subsamples, the distributions are best determined with larger sample sizes. Therefore, for the purposes of averaging the efficiency, only the last three years  $k' = \{2016, 2017, 2018\}$  are used (with distributions quantified as the sum of the weights  $W_{j,k'}$  in each square Dalitz bin  $j$ ), with a given subsample only included if the statistical significance of the signal yield exceeds 2 standard deviations. The only case where this requirement results in a subsample being excluded is in the determination of the  $B_s^0 \rightarrow K_S^0 K^+ K^-$  distribution, where the 2016 LL subsample has an insignificant signal yield ( $1.5 \pm 2.6$ ). Each of these distributions is then corrected for efficiency in bins of the square Dalitz plot; the resulting efficiency-corrected, background-subtracted distribution may then be used to compute the average efficiency for any subsample, including those with smaller yields. The estimate of the weighted-average efficiency for subsample  $k$ , determined using the distribution of subsample  $k'$ , is given by

$$\bar{\epsilon}_{k,k'} = \frac{\sum_j W_{j,k'} \epsilon_{j,k'}^{-1} \epsilon_{j,k}}{\sum_j W_{j,k'} \epsilon_{j,k'}^{-1}}. \quad (6)$$

Note that for each data-taking period  $k$ , there are three independent estimates of the average efficiency, one for each of the reference data-taking periods. These three estimates are then combined, taking the arithmetic mean without weighting (since the three reference data samples are approximately equal in size), to give single efficiency  $\bar{\epsilon}_k$  for each dataset  $k$ .

Known differences between data and simulation are corrected with calibration samples. For the  $h^+$  and  $h'^-$  hadrons, differences in tracking efficiency are corrected as a function of the track momentum and pseudorapidity [64]. An analogous correction is applied to the  $K_S^0$  tracking and vertex-reconstruction efficiency. Differences in hardware-trigger response between data and simulation are determined from samples of  $D^{*+} \rightarrow D^0(\rightarrow K^- \pi^+) \pi^+$  decays triggered by other activity in the event, and are determined as a function of the hadron charge,  $p_T$ , calorimeter region, and the overlap between the calorimeter clusters of the final-state particles in signal decays, including a correction for the average underlying energy in the calorimeter. Differences in particle-identification efficiency and misidentification rates between kaons and pions are determined from the same  $D^{*+}$  calibration samples; as noted in Sec. 3, these corrections are applied before simulated decays are processed by the PID BDT. The tracking-efficiency corrections are of  $\mathcal{O}(1\%)$ , while those related to the trigger efficiency can be up to 10%.

The selection efficiency depends upon the  $b$ -hadron decay-time distribution. In the case of  $B_s^0$  decays, the lifetime difference between the two  $CP$  eigenstates is significant, and at present the  $CP$  content of the three  $B_s^0$  decays is unknown. The  $B_s^0$  decay model used in the simulation assumes an effective lifetime of  $1/\Gamma_s$ , where  $\Gamma_s$  is the average width of the two  $CP$ -eigenstates of the  $B_s^0$  meson. The relative change in the  $CP$ -averaged  $B_s^0$  efficiency corresponding to a variation of the effective  $B_s^0$  meson decay width of  $\pm\Delta\Gamma_s/2$  is estimated to be  $\mp 4\%$ .

## 6 Systematic uncertainties

The branching fractions are measured relative to that of the decay  $B^0 \rightarrow K_S^0 \pi^+ \pi^-$ , as shown in Eq. 5. Similar selections and fit procedures are used for the numerator and denominator, and as a result, many systematic effects cancel at first order in the ratio. The remaining uncertainties are discussed below, grouped according to whether they influence the yield measurements ( $N$ ) or the efficiency ( $\varepsilon$ ); the uncertainty on  $f_s/f_d$  is treated separately. In most cases, systematic uncertainties are first evaluated on the individual measurements (split by data-taking period and  $K_S^0$  reconstruction type); the procedure by which these individual measurements are combined, and the systematic uncertainties on this combination, are discussed in Sec. 6.3.

### 6.1 Fit model and yield measurement uncertainties

Several assumptions are made during the fit procedure, principally the models chosen to describe different components and the choices made when constraining or fixing fit parameters. For each of the 13 assumptions discussed below, the associated systematic uncertainty is evaluated by making a different assumption with respect to the baseline model and rerunning the full analysis up to the determination of the ratios of branching fractions (Eq. 5). The uncertainty on a given ratio for a given subsample is taken to be the absolute value of the difference between the result obtained with the baseline method and with the modified method. This is done separately for each ratio of branching fractions (with  $B_{(s)}^0 \rightarrow K_S^0 K^\pm \pi^\mp$  split by charge), each data-taking period, each  $K_S^0$  reconstruction type, and for the looser and tighter selections (*i.e.* for  $7 \times 7 \times 2 \times 2$  configurations).

For the signal component, systematic uncertainties are assigned based on the two following modifications: replacing the signal model with a double-sided Hypatia function [65], or allowing the mass difference  $\Delta m$  between the  $B^0$  and  $B_s^0$  peaks to vary in the fit.

For the cross-feed component, the two following modifications are considered: the constraint on the ratio of yields of the two cross-feed peaks in each spectrum is removed, allowing them to vary independently; or the yields of cross-feed peaks are allowed to vary instead of being fully constrained when using the tighter selection.

For the partially reconstructed component, fits to representative simulated samples are used to determine the lineshape. In the baseline fit, the charmless decay  $B^0 \rightarrow K^*(892)^0 \rho(770)^0$  is used for  $B^0$  and, with an offset, for  $B_s^0$  decays. In the modified versions, a lineshape derived from fits to a sample of the hadronic decay  $B^+ \rightarrow D^0 \pi^+$ , with  $D^0 \rightarrow K_S^0 \pi^+ \pi^-$ , is considered, first in place of the charmless decay, or second in addition to it. In a third variation, additional components are added to the  $K_S^0 \pi^+ \pi^-$  spectrum to describe radiative decays.

For the combinatorial component, four variations are considered: the slope parameters for the final states  $K_S^0 K^+ \pi^-$  and  $K_S^0 \pi^+ K^-$  are allowed to differ, the slope parameter is allowed to take positive values, the slope parameter is fixed entirely according to a prior fit to the upper mass sideband 5500–5750 MeV/ $c^2$ , or the combinatorial model is replaced with an exponential function.

Finally, in the baseline fit procedure, very small components are suppressed because yields close to the lower bound of zero can cause fit instability: when the fit finds a component yield to be less than one event for a subsample, this is taken to be negligible and fixed to zero, and the data are refitted without that component. This procedure is

instead modified in two ways: by fixing the yield to the fitted value, or by leaving the yield free.

For each subsample and configuration, the procedure above gives a set of 13 fit systematic uncertainties on each ratio of branching fractions. These 13 uncertainties are then combined in quadrature to give an uncertainty on each ratio of branching fractions for the subsample and configuration. These fit uncertainties on the individual subsamples are subsequently propagated, assuming no correlation among the subsamples, to the averaged ratios of branching fractions (see Sec. 6.3). Typically, the largest fit systematic uncertainties arise from fixing the combinatorial slope parameter from a fit to the upper mass sideband, and from using charmed hadronic decays to model the partially reconstructed component.

The systematic uncertainty due to the fit method on the combined yield of  $B_s^0 \rightarrow K_S^0 K^+ K^-$  with the tighter selection is 12. Adding this in quadrature with the statistical uncertainty gives a yield of  $207 \pm 24$ , for which the corresponding significance, based on the ratio of the yield to the total uncertainty, is 8.6 standard deviations.

## 6.2 Efficiency uncertainties

Systematic uncertainties on the efficiency ratios arise from the finite size of the samples of simulated signal events, the accuracy of the corrections for data-simulation differences, and the method used to average the efficiencies.

Uncertainties on the tracking, hardware trigger, and PID corrections arise from the finite size of the data calibration samples. For the hardware-trigger correction, an additional uncertainty arises from the sample with which the average underlying energy is determined; this uncertainty is estimated by remeasuring the average underlying energy with another data calibration sample, using identified charm events instead of identified beauty events. For the PID correction, additional uncertainties arise from the finite size of the simulation sample (used to determine the signal-track kinematic distribution for the correction), and from the nonparametric kernel-density method used to describe the PID response; the latter uncertainty is estimated by varying the kernel width.

In addition, the kinematic distributions of  $B^0$  and  $B_s^0$  mesons may differ between simulation and data; the effect of this is tested by weighting the simulated data to match the kinematic distributions in higher-yield data samples of  $B_{(s)}^0 \rightarrow K_S^0 h^+ h'^-$  decays and recomputing the efficiency. The change in mean efficiency after reweighting is determined for 18 separate subsamples, using combinations of three decay channels ( $B^0 \rightarrow K_S^0 \pi^+ \pi^-$ ,  $B^0 \rightarrow K_S^0 K^+ K^-$ ,  $B_s^0 \rightarrow K_S^0 K^\pm \pi^\mp$ ), three data-taking periods (2016, 2017, 2018), and the two  $K_S^0$  reconstruction types. The effect is found to be small, and a systematic uncertainty is assessed based on the sum in quadrature of the mean and RMS of the 18 subsamples. This uncertainty is taken to be correlated between data-taking periods.

The uncertainty on the method used to compute the weighted-average efficiency  $\bar{\epsilon}_k$  is based on the spread among the three independent estimates  $\bar{\epsilon}_{k,k'}$  (see Eq. 6), quantified as the RMS of  $\{\bar{\epsilon}_{k,k'} - \bar{\epsilon}_k\}$  among all combinations  $k, k'$  for a given decay mode and  $K_S^0$  reconstruction type. (Note that there are  $7 \times 3$  such combinations, for the seven data-taking periods  $k$  and the three reference periods  $k'$ .) While this does mean that some subsamples are reused in the uncertainty estimate it has the important advantage that the systematic uncertainty is stable across data-taking periods and is only mildly affected by statistical fluctuations in the smaller subsamples. This uncertainty is correlated between

data-taking periods.

The average efficiency is also influenced by the choice of binning scheme for the square Dalitz plot. Instead of the baseline  $10 \times 10$  binning, six other  $n \times n$  grids are used (for  $n = 7, 8, 9, 11, 12, 13$ ) and, for each grid, the average efficiency is recomputed and the difference taken with respect to that of the baseline  $n = 10$  grid. This is done for each of the seven data-taking periods, for a total of 42 values, and the RMS of the distribution is taken as an estimate of the associated systematic uncertainty. This generates one uncertainty per decay mode,  $K_S^0$  reconstruction type, and selection working point (looser/tighter), and is thus correlated between data-taking periods.

### 6.3 Combination

For each of the five ratios of branching fractions  $R_i$ , fourteen separate measurements  $R_{ij}$  are made (from the seven data-taking periods and two  $K_S^0$  reconstruction types). In general, the agreement between all of the measurements is excellent. Only a single measurement of one branching fraction ratio shows a significant disagreement with respect to the other thirteen measurements. It is therefore assumed to be due to a fluctuation. The fourteen measurements of each branching fraction ratio are combined in a weighted average:

$$\bar{R}_i = \left[ \sum_j w_{ij} \right]^{-1} \sum_j R_{ij} w_{ij}. \quad (7)$$

The weight used for each measurement is  $w_{ij} = (\sigma_{ij})^{-2}$ , where  $\sigma_{ij}$  is the sum in quadrature of the statistical and uncorrelated systematic uncertainties on the ratio  $R_{ij}$ .

The uncertainties on the individual measurements  $R_{ij}$  are propagated to the combinations  $\bar{R}_i$ . Other than as noted above, systematic uncertainties are assumed to be uncorrelated between subsamples and are added in quadrature. The uncertainties are summarised in Table 2. The largest sources of systematic uncertainty are the modelling of the fit components and the method to account for the efficiency variation over the Dalitz plot.

## 7 Results and conclusion

A dataset recorded by the LHCb detector between 2011 and 2018, corresponding to an integrated luminosity of  $9 \text{ fb}^{-1}$ , is used to study the  $B_{(s)}^0 \rightarrow K_S^0 h^+ h'^-$  decay modes. The branching fraction of each decay is measured relative to that of  $B^0 \rightarrow K_S^0 \pi^+ \pi^-$ . The ratios of branching fractions are determined independently for the two  $K_S^0$  reconstruction categories and seven data-taking periods, with all such determinations being in agreement.

Table 2: Summary of the relative systematic uncertainties on the ratios of branching fractions after taking the weighted average of the subsamples, as described in Sec. 6.3. For each column, the decay mode in the numerator of the ratio of branching fractions is indicated by the initial  $b$  hadron and the  $h^+h^-$  combination. An asterisk indicates that the class includes uncertainties treated as correlated between different data-taking periods.

Source [%]	$B^0, K^+K^-$	$B^0, K^\pm\pi^\mp$	$B_s^0, \pi^+\pi^-$	$B_s^0, K^+K^-$	$B_s^0, K^\pm\pi^\mp$
Fit model	7.8	28.6	40.4	58.8	5.8
Tracking	0.03	0.04	< 0.01	0.07	0.03
Hardware trigger	1.3	1.0	1.0	1.4	0.7
PID	2.3	5.4	< 0.1	6.2	1.8
Kin. reweighting*	6.2	4.4	6.0	6.3	4.4
Dalitz plot*	27.3	22.6	37.3	57.2	15.3
Total systematic	29	37	55	82	17
Statistical	12	26	42	135	11
$f_s/f_d^*$	—	—	31	31	31

They are then combined in a weighted average, and the results obtained are

$$\begin{aligned} \frac{\mathcal{B}(B^0 \rightarrow K_S^0 K^+ K^-)}{\mathcal{B}(B^0 \rightarrow K_S^0 \pi^+ \pi^-)} &= 0.578 \pm 0.007 (\text{stat}) \pm 0.017 (\text{syst}), \\ \frac{\mathcal{B}(B^0 \rightarrow K_S^0 K^\pm \pi^\mp)}{\mathcal{B}(B^0 \rightarrow K_S^0 \pi^+ \pi^-)} &= 0.1363 \pm 0.0035 (\text{stat}) \pm 0.0051 (\text{syst}), \\ \frac{\mathcal{B}(B_s^0 \rightarrow K_S^0 \pi^+ \pi^-)}{\mathcal{B}(B^0 \rightarrow K_S^0 \pi^+ \pi^-)} &= 0.269 \pm 0.011 (\text{stat}) \pm 0.015 (\text{syst}) \pm 0.008 (f_s/f_d), \\ \frac{\mathcal{B}(B_s^0 \rightarrow K_S^0 K^+ K^-)}{\mathcal{B}(B^0 \rightarrow K_S^0 \pi^+ \pi^-)} &= 0.0303 \pm 0.0041 (\text{stat}) \pm 0.0025 (\text{syst}) \pm 0.0009 (f_s/f_d), \\ \frac{\mathcal{B}(B_s^0 \rightarrow K_S^0 K^\pm \pi^\mp)}{\mathcal{B}(B^0 \rightarrow K_S^0 \pi^+ \pi^-)} &= 1.818 \pm 0.021 (\text{stat}) \pm 0.031 (\text{syst}) \pm 0.056 (f_s/f_d). \end{aligned}$$

The decay  $B_s^0 \rightarrow K_S^0 K^+ K^-$  is observed for the first time, with a significance exceeding six standard deviations. All measurements of branching fractions are in good agreement with the earlier LHCb determinations [66], which they supersede. The measurement of the relative branching fractions of  $B^0 \rightarrow K_S^0 K^\pm \pi^\mp$  and  $B^0 \rightarrow K_S^0 K^+ K^-$  are consistent with the world-average results [25, 26]. At present the  $CP$  content of the three  $B_s^0$  decays is unknown but once it is established, *e.g.* by a future amplitude analysis, the branching fraction ratios can be corrected for the modified efficiency within the estimated maximal deviation of  $\pm 4\%$ , corresponding to a variation of the effective  $B_s^0$  meson decay width of  $\mp \Delta\Gamma_s/2$ .

Using the external known value (excluding input from previous LHCb measurements that used a subset of the data considered here),  $\mathcal{B}(B^0 \rightarrow K^0 \pi^+ \pi^-) = (4.96 \pm 0.20) \times$

$10^{-5}$  [26], the measured time-integrated branching fractions are

$$\begin{aligned}
\mathcal{B}(B^0 \rightarrow K^0 K^+ K^-) &= [28.6 \pm 0.4 \text{ (stat)} \pm 0.8 \text{ (syst)} \pm 1.2 \text{ (ext)}] \times 10^{-6}, \\
\mathcal{B}(B^0 \rightarrow K^0 K^\pm \pi^\mp) &= [6.76 \pm 0.17 \text{ (stat)} \pm 0.25 \text{ (syst)} \pm 0.27 \text{ (ext)}] \times 10^{-6}, \\
\mathcal{B}(B_s^0 \rightarrow K^0 \pi^+ \pi^-) &= [13.3 \pm 0.6 \text{ (stat)} \pm 0.7 \text{ (syst)} \pm 0.7 \text{ (ext)}] \times 10^{-6}, \\
\mathcal{B}(B_s^0 \rightarrow K^0 K^+ K^-) &= [1.50 \pm 0.20 \text{ (stat)} \pm 0.12 \text{ (syst)} \pm 0.08 \text{ (ext)}] \times 10^{-6}, \\
\mathcal{B}(B_s^0 \rightarrow K^0 K^\pm \pi^\mp) &= [90.2 \pm 1.0 \text{ (stat)} \pm 1.5 \text{ (syst)} \pm 4.6 \text{ (ext)}] \times 10^{-6},
\end{aligned}$$

where ‘ext’ denotes the combined uncertainties on  $f_s/f_d$  and  $\mathcal{B}(B^0 \rightarrow K^0 \pi^+ \pi^-)$ . These results agree with the available predictions for these channels [4–9], and with previous experimental determinations.

## Acknowledgements

We express our gratitude to our colleagues in the CERN accelerator departments for the excellent performance of the LHC. We thank the technical and administrative staff at the LHCb institutes. We acknowledge support from CERN and from the national agencies: ARC (Australia); CAPES, CNPq, FAPERJ and FINEP (Brazil); MOST and NSFC (China); CNRS/IN2P3 and CEA (France); BMBWF, DFG and MPG (Germany); INFN (Italy); NWO (Netherlands); MNiSW and NCN (Poland); MCID/IFA (Romania); MICIU and AEI (Spain); SNSF and SER (Switzerland); NASU (Ukraine); STFC (United Kingdom); DOE NP and NSF (USA). We acknowledge the computing resources that are provided by ARDC (Australia), CBPF (Brazil), CERN, IHEP and LZU (China), IN2P3 (France), KIT and DESY (Germany), INFN (Italy), SURF (Netherlands), Polish WLCG (Poland), IFIN-HH (Romania), PIC (Spain), CSCS (Switzerland), GridPP (United Kingdom), and NSF (USA). We are indebted to the communities behind the multiple open-source software packages on which we depend. Individual groups or members have received support from Key Research Program of Frontier Sciences of CAS, CAS PIFI, CAS CCEPP (China); Minciencias (Colombia); EPLANET, Marie Skłodowska-Curie Actions, ERC and NextGenerationEU (European Union); A\*MIDEX, ANR, IPhU and Labex P2IO, and Région Auvergne-Rhône-Alpes (France); Alexander-von-Humboldt Foundation (Germany); ICSC (Italy); Severo Ochoa and María de Maeztu Units of Excellence, GVA, XuntaGal, GENCAT, InTalent-Inditex and Prog. Atracción Talento CM (Spain); the Leverhulme Trust, the Royal Society and UKRI (United Kingdom).

# Appendices

## A Fits to all subsamples

For each ratio of branching fractions, 14 separate measurements  $R_{ij}$  are made and a weighted average  $\bar{R}_i$  is computed, as described in Sec. 6.3. The same set of measurements may also be used to compute a  $\chi^2$ ,

$$\chi_i^2 = \sum_j \left( \frac{R_{ij} - \bar{R}_i}{\sigma_{ij}} \right)^2, \quad (8)$$

where  $\sigma_{ij}$  is the sum in quadrature of the statistical and uncorrelated systematic uncertainties on the ratio  $R_{ij}$ , implicitly assuming Gaussian uncertainties. The results are given in Table 3, along with the associated  $p$ -values. All indicate good agreement, except for the ratio  $\mathcal{B}(B_s^0 \rightarrow K_S^0 K^+ K^-)/\mathcal{B}(B^0 \rightarrow K_S^0 \pi^+ \pi^-)$ . For the latter, the largest contribution (9.6) comes from the 2016 data-taking period with the long  $K_S^0$  reconstruction type; all other subsamples are mutually consistent (the remaining  $\chi^2/\text{ndf}$  would be 19.84/13, corresponding to a  $p$ -value of 10%). The fit to the  $K_S^0 K^+ K^-$  spectrum for this sample is shown in Fig. 3. In this instance, both the fitted yield of  $B_s^0 \rightarrow K_S^0 K^+ K^-$  ( $1.5 \pm 2.6$  candidates) and the background in the peak region are small, with the consequence that the estimated statistical uncertainty is also low, enhancing the  $\chi^2$  contribution. This effect is reproduced in simulated pseudoexperiments emulating the 2016 LL  $K_S^0 K^+ K^-$  mass spectrum, in which the  $B_s^0$  signal yield is drawn from a Poisson distribution where the expected signal yield is determined from the branching ratio averaged across all subsamples, and expected yields of other components are taken from the fit to data. In fits to the pseudoexperiments, downward fluctuations in the fitted  $B_s^0$  yield are found to be correlated with lower statistical uncertainties on the yield, and hence larger normalised residuals (pulls), with the effect becoming strongly nonlinear for fitted yields in this spectrum below five units.

Table 3: For each measured ratio of branching fractions, the estimated  $\chi^2$  for compatibility among subsamples, the associated number of degrees of freedom (ndf), and the corresponding  $p$ -value assuming Gaussian uncertainties.

Ratio	$\chi^2/\text{ndf}$	$p$ -value
$\mathcal{B}(B^0 \rightarrow K_S^0 K^+ K^-)/\mathcal{B}(B^0 \rightarrow K_S^0 \pi^+ \pi^-)$	17.9/13	16%
$\mathcal{B}(B^0 \rightarrow K_S^0 K^\pm \pi^\mp)/\mathcal{B}(B^0 \rightarrow K_S^0 \pi^+ \pi^-)$	6.91/13	91%
$\mathcal{B}(B_s^0 \rightarrow K_S^0 \pi^+ \pi^-)/\mathcal{B}(B^0 \rightarrow K_S^0 \pi^+ \pi^-)$	10.5/13	65%
$\mathcal{B}(B_s^0 \rightarrow K_S^0 K^+ K^-)/\mathcal{B}(B^0 \rightarrow K_S^0 \pi^+ \pi^-)$	33.0/13	0.17%
$\mathcal{B}(B_s^0 \rightarrow K_S^0 K^\pm \pi^\mp)/\mathcal{B}(B^0 \rightarrow K_S^0 \pi^+ \pi^-)$	9.50/13	73%

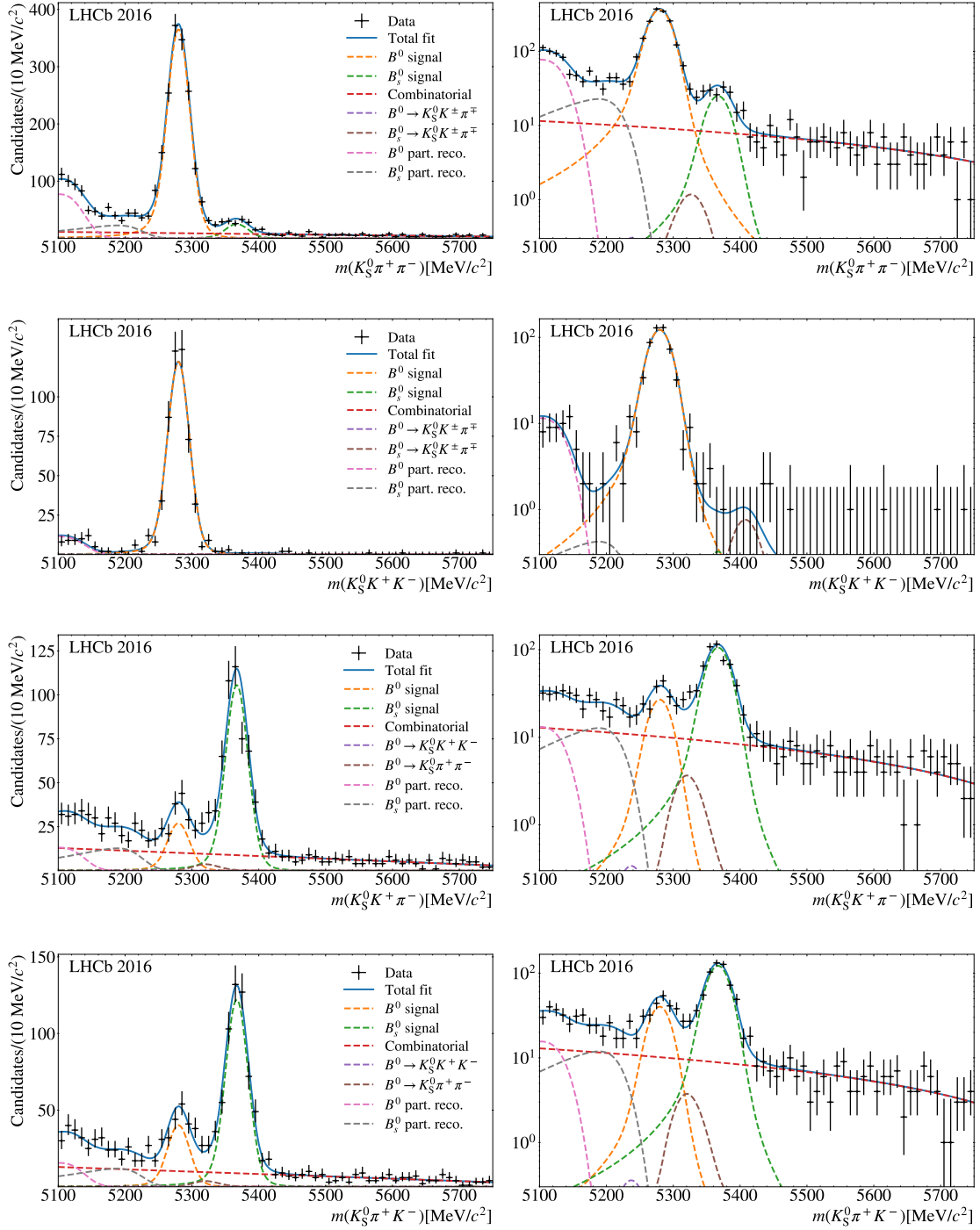


Figure 3: Mass distributions of  $K_S^0 h^+ h^-$  candidates that pass the tighter selection, for the 2016 running period and the long  $K_S^0$  reconstruction type. From top to bottom, each row corresponds to a different final state:  $K_S^0 \pi^+ \pi^-$ ,  $K_S^0 K^+ K^-$ ,  $K_S^0 K^+ \pi^-$ ,  $K_S^0 \pi^+ K^-$ .

## B Definition of the signal model

In this analysis, the probability density function (PDF) of a Crystal Ball function [56], as implemented in ROOFIT within ROOT [67], is defined as follows:

$$P_{\text{CB}}(m; \mu, \sigma, n, \alpha) \equiv N \begin{cases} e^{-t^2/2} & \text{if } t > -|\alpha|, \\ \frac{1}{\left(\frac{n}{|\alpha|} - |\alpha| - t\right)^n} \left(\frac{n}{|\alpha|}\right)^n e^{-\alpha^2/2} & \text{if } t \leq -|\alpha|, \end{cases} \quad (9)$$

where

$$t = \begin{cases} (m - \mu)/\sigma & \text{if } \alpha > 0, \\ -(m - \mu)/\sigma & \text{if } \alpha < 0, \end{cases} \quad (10)$$

and where  $N$  is a normalisation factor such that the PDF has unit integral within the fit range. The signal PDF is then defined as

$$P_{\text{sig}}(m; \mu, \sigma, n_L, n_R, \alpha_L, \alpha_R, f_L) \equiv f_L P_{\text{CB}}(m; \mu, \sigma, n_L, \alpha_L) + (1 - f_L) P_{\text{CB}}(m; \mu, \sigma, n_R, -\alpha_R). \quad (11)$$

Fits to signal candidates in simulation are used to obtain a set of signal shape parameters, some of which are used in the fit to data as described below. Simultaneous fits are used to share parameters between different decay modes and different  $K_S^0$  reconstruction types for a given data-taking period (but not between different data-taking periods). The 22 shape parameters determined for each data-taking period are:

- Two peak position parameters  $\mu(B^0)$  and  $\mu(B_s^0)$ ;
- One width parameter  $\sigma(B^0 \rightarrow K_S^0 \pi^+ \pi^-, \text{DD})$  for the decay  $B^0 \rightarrow K_S^0 \pi^+ \pi^-$  with the downstream  $K_S^0$  reconstruction;
- Four width ratio parameters,  $\{r_{B_s^0}, r_{K\pi}, r_{KK}, r_{LL}\}$ , which together define the width of the other signal peaks relative to  $\sigma(B^0 \rightarrow K_S^0 \pi^+ \pi^-, \text{DD})$  under the assumption of factorisation:

$$\begin{aligned} \sigma(B_s^0 \rightarrow K_S^0 \pi^+ \pi^-, \text{DD}) &= \sigma(B^0 \rightarrow K_S^0 \pi^+ \pi^-, \text{DD}) r_{B_s^0}, \\ \sigma(B^0 \rightarrow K_S^0 \pi^+ \pi^-, \text{LL}) &= \sigma(B^0 \rightarrow K_S^0 \pi^+ \pi^-, \text{DD}) r_{LL}, \\ \sigma(B_s^0 \rightarrow K_S^0 \pi^+ \pi^-, \text{LL}) &= \sigma(B^0 \rightarrow K_S^0 \pi^+ \pi^-, \text{DD}) r_{B_s^0} r_{LL}, \\ \sigma(B^0 \rightarrow K_S^0 K^\pm \pi^\mp, \text{DD}) &= \sigma(B^0 \rightarrow K_S^0 \pi^+ \pi^-, \text{DD}) r_{K\pi}, \\ \sigma(B_s^0 \rightarrow K_S^0 K^\pm \pi^\mp, \text{DD}) &= \sigma(B^0 \rightarrow K_S^0 \pi^+ \pi^-, \text{DD}) r_{B_s^0} r_{K\pi}, \\ \sigma(B^0 \rightarrow K_S^0 K^\pm \pi^\mp, \text{LL}) &= \sigma(B^0 \rightarrow K_S^0 \pi^+ \pi^-, \text{DD}) r_{K\pi} r_{LL}, \\ \sigma(B_s^0 \rightarrow K_S^0 K^\pm \pi^\mp, \text{LL}) &= \sigma(B^0 \rightarrow K_S^0 \pi^+ \pi^-, \text{DD}) r_{B_s^0} r_{K\pi} r_{LL}, \\ \sigma(B^0 \rightarrow K_S^0 K^+ K^-, \text{DD}) &= \sigma(B^0 \rightarrow K_S^0 \pi^+ \pi^-, \text{DD}) r_{KK}, \\ \sigma(B_s^0 \rightarrow K_S^0 K^+ K^-, \text{DD}) &= \sigma(B^0 \rightarrow K_S^0 \pi^+ \pi^-, \text{DD}) r_{B_s^0} r_{KK}, \\ \sigma(B^0 \rightarrow K_S^0 K^+ K^-, \text{LL}) &= \sigma(B^0 \rightarrow K_S^0 \pi^+ \pi^-, \text{DD}) r_{KK} r_{LL}, \\ \sigma(B_s^0 \rightarrow K_S^0 K^+ K^-, \text{LL}) &= \sigma(B^0 \rightarrow K_S^0 \pi^+ \pi^-, \text{DD}) r_{B_s^0} r_{KK} r_{LL}; \end{aligned}$$

- Six left-hand tail parameters, which are different between final states but shared between  $K_S^0$  reconstruction types and between the  $B^0$  and  $B_s^0$  peaks for a given final state:  $\{\alpha_L(K_S^0 \pi^+ \pi^-), \alpha_L(K_S^0 K^\pm \pi^\mp), \alpha_L(K_S^0 K^+ K^-)\}$  and  $\{n_L(K_S^0 \pi^+ \pi^-), n_L(K_S^0 K^\pm \pi^\mp), n_L(K_S^0 K^+ K^-)\}$ ;

- Six parameters to define the right-hand tail, each expressed as a ratio with respect to the corresponding left-hand tail parameter give above, *e.g.*  $\alpha_R(K_S^0\pi^+\pi^-)/\alpha_L(K_S^0\pi^+\pi^-)$ , and which are likewise different between final states but shared between  $K_S^0$  reconstruction types and between the  $B^0$  and  $B_s^0$  peaks for a given final state;
- Three parameters describing the fraction of the signal in the component with the left-hand tail, which are different between final states but shared between  $K_S^0$  reconstruction types and between the  $B^0$  and  $B_s^0$  peaks for a given final state:  $\{f_L(K_S^0\pi^+\pi^-), f_L(K_S^0K^\pm\pi^\mp), f_L(K_S^0K^+K^-)\}$ .

In the simultaneous fits to data, for each data-taking period most shape parameters are fixed according to the corresponding fits to simulation. Specifically, all of the width ratio parameters ( $r$ ), all of the tail parameters ( $n_L, n_R, \alpha_L, \alpha_R$ ), and all of the fraction parameters ( $f_L$ ) are fixed. The width parameter  $\sigma(B^0 \rightarrow K_S^0\pi^+\pi^-, \text{DD})$  is allowed to vary, to take into account potential differences in resolution between data and simulation. Similarly, one peak position parameter  $\mu(B^0)$  is allowed to vary so as to take into account potential differences in mass scale between data and simulation; the other peak position parameter is then derived as  $\mu(B_s^0) = \mu(B^0) + \Delta m$ , where  $\Delta m$  is fixed to the known difference in mass between the two states [26]. All 16 signal yields (for the four final states with  $K_S^0K^+\pi^-$  and  $K_S^0\pi^+K^-$  separated by charge, two  $K_S^0$  reconstruction types, and  $B^0$  and  $B_s^0$ ) for each data-taking period are free parameters.

Note that the fits described above are carried out separately at the two selection working points (loose and tight), since signal shapes and yields depend upon the selection.

## C Correlation matrices

### C.1 Statistical correlation matrix

The statistical correlations between the ratios of branching fractions are reported in Table 4. Some branching fraction results are determined from the tight selection and others from the loose selection. The correlation matrix is computed from the tight selection, since those data are a subsample of those in the loose selection.

The correlation among yields is obtained directly from the fit and is found to be low (below 1% for most cases). Then the correlation is propagated to the ratio of yields and finally to the ratio of branching fractions. The final correlation obtained mainly results from the common denominator decay mode  $B^0 \rightarrow K_S^0\pi^+\pi^-$ .

Table 4: Statistical correlations, calculated as described in the text, between the ratios of branching fractions  $\mathcal{B}(B_{(s)}^0 \rightarrow K_S^0 h^+ h'^-)/\mathcal{B}(B^0 \rightarrow K_S^0\pi^+\pi^-)$ , where the numerator decay mode is given by the row and column headings.

	$B^0 \rightarrow K_S^0 K^+ K^-$	$B^0 \rightarrow K_S^0 K^\pm \pi^\mp$	$B_s^0 \rightarrow K_S^0 \pi^+ \pi^-$	$B_s^0 \rightarrow K_S^0 K^+ K^-$	$B_s^0 \rightarrow K_S^0 K^\pm \pi^\mp$
$B^0 \rightarrow K_S^0 K^+ K^-$	1.00	0.16	0.06	0.03	0.33
$B^0 \rightarrow K_S^0 K^\pm \pi^\mp$	0.16	1.00	0.04	0.01	0.29
$B_s^0 \rightarrow K_S^0 \pi^+ \pi^-$	0.06	0.04	1.00	0.006	0.07
$B_s^0 \rightarrow K_S^0 K^+ K^-$	0.03	0.01	0.006	1.00	0.03
$B_s^0 \rightarrow K_S^0 K^\pm \pi^\mp$	0.33	0.29	0.07	0.03	1.00

Table 5: Statistical covariance matrix between the ratios of branching fractions  $\mathcal{B}(B_{(s)}^0 \rightarrow K_S^0 h^+ h^-) / \mathcal{B}(B^0 \rightarrow K_S^0 \pi^+ \pi^-)$ , where the numerator decay mode is given by the row and column headings.

	$B^0 \rightarrow K_S^0 K^+ K^-$	$B^0 \rightarrow K_S^0 K^\pm \pi^\mp$	$B_s^0 \rightarrow K_S^0 \pi^+ \pi^-$	$B_s^0 \rightarrow K_S^0 K^+ K^-$	$B_s^0 \rightarrow K_S^0 K^\pm \pi^\mp$	
$B^0 \rightarrow K_S^0 K^+ K^-$	5.11	0.39	0.51	0.09	4.83	) $\times 10^{-5}$
$B^0 \rightarrow K_S^0 K^\pm \pi^\mp$	0.39	1.21	0.17	0.02	2.10	
$B_s^0 \rightarrow K_S^0 \pi^+ \pi^-$	0.51	0.17	12.68	0.03	1.63	
$B_s^0 \rightarrow K_S^0 K^+ K^-$	0.09	0.02	0.03	1.67	0.24	
$B_s^0 \rightarrow K_S^0 K^\pm \pi^\mp$	4.83	2.10	1.63	0.24	42.81	

The statistical covariance matrix is shown in Table 5. It is obtained from Table 4 using the statistical uncertainties on branching fractions reported in Sec. 7.

## C.2 Correlation matrices due to the efficiency binning scheme

Among the considered sources of systematic correlation, only the contribution associated with the efficiency-binning scheme is found to be significant. All other sources can be considered to be negligible. Since similar resonances appear in the different decays, a change in the Dalitz-plot efficiency binning might induce coherent shifts in the efficiency ratios of different signal modes, leading to correlated variations in the corresponding branching-fraction observables. In addition, the variation in the normalisation channel is common to all the ratios.

The correlations among the different signal modes due to the binning of the efficiency variation over the Dalitz plot are evaluated from the changes induced when the binning scheme is modified. For each signal mode an efficiency ratio with respect to the reference channel,  $B^0 \rightarrow K_S^0 \pi^+ \pi^-$ , is formed in every alternative binning, data-taking period, and  $K_S^0$  reconstruction category, and the deviation of this ratio with respect to the baseline  $10 \times 10$  binning is considered. For each pair of modes, all these deviations (over all binning schemes and subsamples) are treated as a sample from which the Pearson correlation coefficient is computed; these values are used as the correlation coefficients for the binning systematic and are reported in Tables 6 and 7 for the tight and loose selections, respectively. The statistical uncertainties on the coefficients are obtained from the standard Fisher  $z$ -transform and quoted as  $\rho_{ij} \pm \sigma_{\rho_{ij}}$ . For modes that differ only by the kaon-pion charge assignment, the two-charge configurations are first averaged, so that the matrices are expressed in terms of combined  $K_S^0 K \pi$  observables.

Finally, to obtain the covariance matrices from the correlation matrices in Tables 6 and 7, the binning-scheme systematic uncertainties propagated to the combined branching fraction ratios are used. The resulting covariance matrices for the tighter and looser optimizations are reported in Tables 8 and 9, respectively.

To obtain the systematic covariance between two branching fractions computed in the looser selection (e.g.  $B^0 \rightarrow K_S^0 K^+ K^-$  and  $B_s^0 \rightarrow K_S^0 K^\pm \pi^\mp$ ), the matrix in Table 9 should be used. If both branching fractions are computed in the tighter selection (e.g.  $B^0 \rightarrow K_S^0 K^\pm \pi^\mp$  and  $B_s^0 \rightarrow K_S^0 K^+ K^-$ ), the matrix in Table 8 should be used. To obtain the covariance between one branching fraction computed in the looser selection and another computed in the tighter selection (e.g.  $B^0 \rightarrow K_S^0 K^+ K^-$  and  $B_s^0 \rightarrow K_S^0 K^\pm \pi^\mp$ ), the matrix in Table 8 is used as an approximation for simplicity.

Table 6: Correlation matrix due to the efficiency binning scheme for the tighter selection between the ratios of efficiencies  $\varepsilon_{B(s)}^{\text{sel}} \rightarrow K_S^0 h^+ h'^- / \varepsilon_{B^0}^{\text{sel}} \rightarrow K_S^0 \pi^+ \pi^-$ , where the numerator decay mode is given by the row and column headings.

$$\begin{array}{l}
B^0 \rightarrow K_S^0 K^+ K^- \\
B^0 \rightarrow K_S^0 K^\pm \pi^\mp \\
B_s^0 \rightarrow K_S^0 \pi^+ \pi^- \\
B_s^0 \rightarrow K_S^0 K^+ K^- \\
B_s^0 \rightarrow K_S^0 K^\pm \pi^\mp
\end{array}
\begin{pmatrix}
B^0 \rightarrow K_S^0 K^+ K^- & B^0 \rightarrow K_S^0 K^\pm \pi^\mp & B_s^0 \rightarrow K_S^0 \pi^+ \pi^- & B_s^0 \rightarrow K_S^0 K^+ K^- & B_s^0 \rightarrow K_S^0 K^\pm \pi^\mp \\
1.00 & 0.40 \pm 0.09 & 0.09 \pm 0.11 & 0.26 \pm 0.10 & 0.33 \pm 0.10 \\
0.40 \pm 0.09 & 1.00 & -0.14 \pm 0.11 & -0.04 \pm 0.11 & 0.53 \pm 0.08 \\
0.09 \pm 0.11 & -0.14 \pm 0.11 & 1.00 & -0.19 \pm 0.11 & -0.05 \pm 0.11 \\
0.26 \pm 0.10 & -0.04 \pm 0.11 & -0.19 \pm 0.11 & 1.00 & 0.34 \pm 0.10 \\
0.33 \pm 0.10 & 0.53 \pm 0.08 & -0.05 \pm 0.11 & 0.34 \pm 0.10 & 1.00
\end{pmatrix}$$

Table 7: Correlation matrix due to the efficiency binning scheme for the looser selection between the ratios of efficiencies  $\varepsilon_{B(s)}^{\text{sel}} \rightarrow K_S^0 h^+ h'^- / \varepsilon_{B^0}^{\text{sel}} \rightarrow K_S^0 \pi^+ \pi^-$ , where the numerator decay mode is given by the row and column headings.

$$\begin{array}{l}
B^0 \rightarrow K_S^0 K^+ K^- \\
B^0 \rightarrow K_S^0 K^\pm \pi^\mp \\
B_s^0 \rightarrow K_S^0 \pi^+ \pi^- \\
B_s^0 \rightarrow K_S^0 K^+ K^- \\
B_s^0 \rightarrow K_S^0 K^\pm \pi^\mp
\end{array}
\begin{pmatrix}
B^0 \rightarrow K_S^0 K^+ K^- & B^0 \rightarrow K_S^0 K^\pm \pi^\mp & B_s^0 \rightarrow K_S^0 \pi^+ \pi^- & B_s^0 \rightarrow K_S^0 K^+ K^- & B_s^0 \rightarrow K_S^0 K^\pm \pi^\mp \\
1.00 & 0.49 \pm 0.08 & 0.05 \pm 0.11 & 0.22 \pm 0.11 & 0.50 \pm 0.08 \\
0.49 \pm 0.08 & 1.00 & -0.16 \pm 0.11 & -0.06 \pm 0.11 & 0.65 \pm 0.06 \\
0.05 \pm 0.11 & -0.16 \pm 0.11 & 1.00 & -0.17 \pm 0.11 & -0.09 \pm 0.11 \\
0.22 \pm 0.11 & -0.06 \pm 0.11 & -0.17 \pm 0.11 & 1.00 & 0.37 \pm 0.10 \\
0.50 \pm 0.08 & 0.65 \pm 0.06 & -0.09 \pm 0.11 & 0.37 \pm 0.10 & 1.00
\end{pmatrix}$$

Table 8: Covariance matrix due to the efficiency binning scheme for the tighter selection between the ratios of efficiencies  $\varepsilon_{B(s)}^{\text{sel}} \rightarrow K_S^0 h^+ h'^- / \varepsilon_{B^0}^{\text{sel}} \rightarrow K_S^0 \pi^+ \pi^-$ , where the numerator decay mode is given by the row and column headings.

$$\begin{array}{l}
B^0 \rightarrow K_S^0 K^+ K^- \\
B^0 \rightarrow K_S^0 K^\pm \pi^\mp \\
B_s^0 \rightarrow K_S^0 \pi^+ \pi^- \\
B_s^0 \rightarrow K_S^0 K^+ K^- \\
B_s^0 \rightarrow K_S^0 K^\pm \pi^\mp
\end{array}
\begin{pmatrix}
B^0 \rightarrow K_S^0 K^+ K^- & B^0 \rightarrow K_S^0 K^\pm \pi^\mp & B_s^0 \rightarrow K_S^0 \pi^+ \pi^- & B_s^0 \rightarrow K_S^0 K^+ K^- & B_s^0 \rightarrow K_S^0 K^\pm \pi^\mp \\
16.83 & 1.16 & 0.50 & 0.35 & 10.35 \\
1.16 & 0.50 & -0.14 & -0.01 & 2.88 \\
0.50 & -0.14 & 1.87 & -0.09 & -0.49 \\
0.35 & -0.01 & -0.09 & 0.11 & 0.88 \\
10.35 & 2.88 & -0.49 & 0.88 & 58.86
\end{pmatrix} \times 10^{-5}$$

Table 9: Covariance matrix due to the efficiency binning scheme for the looser selection between the ratios of efficiencies  $\varepsilon_{B(s)}^{\text{sel}} \rightarrow K_S^0 h^+ h'^- / \varepsilon_{B^0}^{\text{sel}} \rightarrow K_S^0 \pi^+ \pi^-$ , where the numerator decay mode is given by the row and column headings.

$$\begin{array}{l}
B^0 \rightarrow K_S^0 K^+ K^- \\
B^0 \rightarrow K_S^0 K^\pm \pi^\mp \\
B_s^0 \rightarrow K_S^0 \pi^+ \pi^- \\
B_s^0 \rightarrow K_S^0 K^+ K^- \\
B_s^0 \rightarrow K_S^0 K^\pm \pi^\mp
\end{array}
\begin{pmatrix}
B^0 \rightarrow K_S^0 K^+ K^- & B^0 \rightarrow K_S^0 K^\pm \pi^\mp & B_s^0 \rightarrow K_S^0 \pi^+ \pi^- & B_s^0 \rightarrow K_S^0 K^+ K^- & B_s^0 \rightarrow K_S^0 K^\pm \pi^\mp \\
15.14 & 1.09 & 0.25 & 0.37 & 9.70 \\
1.09 & 0.33 & -0.11 & -0.01 & 1.84 \\
0.25 & -0.11 & 1.57 & -0.09 & -0.55 \\
0.37 & -0.01 & -0.09 & 0.18 & 0.77 \\
9.70 & 1.84 & -0.55 & 0.77 & 24.72
\end{pmatrix} \times 10^{-5}$$

## References

- [1] Y. Grossman and M. P. Worah, *CP asymmetries in B decays with new physics in decay amplitudes*, *Phys. Lett.* **B395** (1997) 241, [arXiv:hep-ph/9612269](#).
- [2] D. London and A. Soni, *Measuring the CP angle  $\beta$  in hadronic  $b \rightarrow s$  penguin decays*, *Phys. Lett.* **B407** (1997) 61, [arXiv:hep-ph/9704277](#).
- [3] M. Ciuchini *et al.*, *CP violating B decays in the standard model and supersymmetry*, *Phys. Rev. Lett.* **79** (1997) 978, [arXiv:hep-ph/9704274](#).
- [4] H.-Y. Cheng and C.-K. Chua, *Branching fractions and direct CP violation in charmless three-body decays of B mesons*, *Phys. Rev.* **D88** (2013) 114014, [arXiv:1308.5139](#).
- [5] H.-Y. Cheng and C.-K. Chua, *Charmless three-body decays of  $B_s^0$  mesons*, *Phys. Rev.* **D89** (2014) 074025, [arXiv:1401.5514](#).
- [6] Y. Li, *Branching fractions and direct CP asymmetries of  $\bar{B}_s^0 \rightarrow K^0 h^+ h'^- (h^{(\prime)} = K, \pi)$  decays*, *Sci. China Phys. Mech. Astron.* **58** (2015) 031001, [arXiv:1401.5948](#).
- [7] Y. Li, *Comprehensive study of  $\bar{B}^0 \rightarrow K^0(\bar{K}^0)K^\mp\pi^\pm$  decays in the factorization approach*, *Phys. Rev.* **D89** (2014) 094007, [arXiv:1402.6052](#).
- [8] W.-F. Wang and H.-n. Li, *Quasi-two-body decays  $B \rightarrow K\rho \rightarrow K\pi\pi$  in perturbative QCD approach*, *Phys. Lett.* **B763** (2016) 29, [arXiv:1609.04614](#).
- [9] Y. Li, A.-J. Ma, W.-F. Wang, and Z.-J. Xiao, *Quasi-two-body decays  $B_{(s)} \rightarrow P\rho'(1450), P\rho''(1700) \rightarrow P\pi\pi$  in the perturbative QCD approach*, *Phys. Rev.* **D96** (2017) 036014, [arXiv:1704.07566](#).
- [10] X.-G. He, G.-N. Li, and D. Xu,  *$SU(3)$  and isospin breaking effects on  $B \rightarrow PPP$  amplitudes*, *Phys. Rev.* **D91** (2015) 014029, [arXiv:1410.0476](#).
- [11] Belle collaboration, A. Garmash *et al.*, *Study of B meson decays to three body charmless hadronic final states*, *Phys. Rev.* **D69** (2004) 012001, [arXiv:hep-ex/0307082](#).
- [12] Belle collaboration, A. Garmash *et al.*, *Dalitz analysis of three-body charmless  $B^0 \rightarrow K^0\pi^+\pi^-$  decay*, *Phys. Rev.* **D75** (2007) 012006, [arXiv:hep-ex/0610081](#).
- [13] BaBar collaboration, B. Aubert *et al.*, *Time-dependent amplitude analysis of  $B^0 \rightarrow K_S^0\pi^+\pi^-$* , *Phys. Rev.* **D80** (2009) 112001, [arXiv:0905.3615](#).
- [14] BaBar collaboration, P. del Amo Sanchez *et al.*, *Observation of the rare decay  $B^0 \rightarrow K_S^0 K^\pm\pi^\mp$* , *Phys. Rev.* **D82** (2010) 031101, [arXiv:1003.0640](#).
- [15] BaBar collaboration, J. P. Lees *et al.*, *Study of CP violation in Dalitz-plot analyses of  $B^0 \rightarrow K_S^0 K^+ K^-$ ,  $B^+ \rightarrow K^+ K^- K^+$ , and  $B^+ \rightarrow K_S^0 K_S^0 K^+$* , *Phys. Rev.* **D85** (2012) 112010, [arXiv:1201.5897](#).
- [16] LHCb collaboration, R. Aaij *et al.*, *Study of  $B_{(s)}^0 \rightarrow K_S^0 h^+ h'^-$  decays with first observation of  $B_s^0 \rightarrow K_S^0 K^\pm\pi^\mp$  and  $B_s^0 \rightarrow K_S^0\pi^+\pi^-$* , *JHEP* **10** (2013) 143, [arXiv:1307.7648](#).

- [17] LHCb collaboration, R. Aaij *et al.*, *Updated branching fraction measurements of  $B_{(s)}^0 \rightarrow K_S^0 h^+ h'^-$  decays*, *JHEP* **11** (2017) 027, [arXiv:1707.01665](#).
- [18] N. Cabibbo, *Unitary symmetry and leptonic decays*, *Phys. Rev. Lett.* **10** (1963) 531.
- [19] M. Kobayashi and T. Maskawa, *CP-violation in the renormalizable theory of weak interaction*, *Prog. Theor. Phys.* **49** (1973) 652.
- [20] M. Beneke, *Corrections to  $\sin(2\beta)$  from CP asymmetries in  $B^0 \rightarrow (\pi^0, \rho^0, \eta, \eta', \omega, \phi) K_S^0$  decays*, *Phys. Lett.* **B620** (2005) 143, [arXiv:hep-ph/0505075](#).
- [21] G. Buchalla, G. Hiller, Y. Nir, and G. Raz, *The pattern of CP asymmetries in  $b \rightarrow s$  transitions*, *JHEP* **09** (2005) 074, [arXiv:hep-ph/0503151](#).
- [22] R. Dutta and S. Gardner, *CP asymmetries in  $B \rightarrow f_0 K_S^0$  decays*, *Phys. Rev.* **D78** (2008) 034021, [arXiv:0805.1963](#).
- [23] Belle collaboration, J. Dalseno *et al.*, *Time-dependent Dalitz plot measurement of CP parameters in  $B^0 \rightarrow K_S^0 \pi^+ \pi^-$  decays*, *Phys. Rev.* **D79** (2009) 072004, [arXiv:0811.3665](#).
- [24] Belle collaboration, Y. Nakahama *et al.*, *Measurement of CP violating asymmetries in  $B^0 \rightarrow K_S^0 K^+ K^-$  decays with a time-dependent Dalitz approach*, *Phys. Rev.* **D82** (2010) 073011, [arXiv:1007.3848](#).
- [25] Heavy Flavor Averaging Group, S. Banerjee *et al.*, *Averages of b-hadron, c-hadron, and  $\tau$ -lepton properties as of 2023*, *Phys. Rev.* **D113** (2026) 012008, [arXiv:2411.18639](#).
- [26] Particle Data Group, S. Navas *et al.*, *Review of particle physics*, *Phys. Rev.* **D110** (2024) 030001.
- [27] M. Ciuchini, M. Pierini, and L. Silvestrini,  *$B_s^0 \rightarrow K^{(*)0} \bar{K}^{(*)0}$  decays: the golden channels for new physics searches*, *Phys. Rev. Lett.* **100** (2008) 031802, [arXiv:hep-ph/0703137](#).
- [28] M. Ciuchini, M. Pierini, and L. Silvestrini, *New bounds on the CKM matrix from  $B \rightarrow K \pi \pi$  Dalitz plot analyses*, *Phys. Rev.* **D74** (2006) 051301, [arXiv:hep-ph/0601233](#).
- [29] M. Gronau, D. Pirjol, A. Soni, and J. Zupan, *Improved method for CKM constraints in charmless three-body  $B$  and  $B_s^0$  decays*, *Phys. Rev.* **D75** (2007) 014002, [arXiv:hep-ph/0608243](#).
- [30] CKMfitter group, J. Charles, S. Descotes-Genon, J. Ocariz, and A. Pérez Pérez, *Disentangling weak and strong interactions in  $B \rightarrow K^*(\rightarrow K \pi) \pi$  Dalitz-plot analyses*, *Eur. Phys. J* **C77** (2017) 561, [arXiv:1704.01596](#).
- [31] BaBar collaboration, J. P. Lees *et al.*, *Amplitude analysis of  $B^0 \rightarrow K^+ \pi^- \pi^0$  and evidence of direct CP violation in  $B \rightarrow K^* \pi$  decays*, *Phys. Rev.* **D83** (2011) 112010, [arXiv:1105.0125](#).

- [32] BaBar collaboration, J. P. Lees *et al.*, *Evidence for CP violation in  $B^+ \rightarrow K^*(892)^+\pi^0$  from a Dalitz plot analysis of  $B^+ \rightarrow K_S^0\pi^+\pi^0$  decays*, *Phys. Rev.* **D96** (2017) 072001, [arXiv:1501.00705](#).
- [33] N. Rey-Le Lorier and D. London, *Measuring  $\gamma$  with  $B \rightarrow K\pi\pi$  and  $B \rightarrow KK\bar{K}$  decays*, *Phys. Rev.* **D85** (2012) 016010, [arXiv:1109.0881](#).
- [34] B. Bhattacharya, M. Imbeault, and D. London, *Extraction of the CP-violating phase  $\gamma$  using  $B \rightarrow K\pi\pi$  and  $B \rightarrow KK\bar{K}$  decays*, *Phys. Lett.* **B728** (2014) 206, [arXiv:1303.0846](#).
- [35] B. Bhattacharya and D. London, *Using U spin to extract  $\gamma$  from charmless  $B \rightarrow PPP$  decays*, *JHEP* **04** (2015) 154, [arXiv:1503.00737](#).
- [36] E. Bertholet *et al.*, *Extraction of the CKM phase  $\gamma$  using charmless 3-body decays of B mesons*, *Phys. Rev.* **D99** (2019) 114011, [arXiv:1812.06194](#).
- [37] M. Ciuchini, M. Pierini, and L. Silvestrini, *Hunting the CKM weak phase with time-integrated Dalitz analyses of  $B_s^0 \rightarrow K\pi\pi$  decays*, *Phys. Lett.* **B645** (2007) 201, [arXiv:hep-ph/0602207](#).
- [38] LHCb collaboration, R. Aaij *et al.*, *Measurement of the b-quark production cross-section in 7 and 13 TeV pp collisions*, *Phys. Rev. Lett.* **118** (2017) 052002, Erratum *ibid.* **119** (2017) 169901, [arXiv:1612.05140](#).
- [39] K. De Bruyn *et al.*, *Branching ratio measurements of  $B_s^0$  decays*, *Phys. Rev.* **D86** (2012) 014027, [arXiv:1204.1735](#).
- [40] LHCb collaboration, A. A. Alves Jr. *et al.*, *The LHCb detector at the LHC*, *JINST* **3** (2008) S08005.
- [41] LHCb collaboration, R. Aaij *et al.*, *LHCb detector performance*, *Int. J. Mod. Phys.* **A30** (2015) 1530022, [arXiv:1412.6352](#).
- [42] T. Sjöstrand, S. Mrenna, and P. Skands, *A brief introduction to PYTHIA 8.1*, *Comput. Phys. Commun.* **178** (2008) 852, [arXiv:0710.3820](#); T. Sjöstrand, S. Mrenna, and P. Skands, *PYTHIA 6.4 physics and manual*, *JHEP* **05** (2006) 026, [arXiv:hep-ph/0603175](#).
- [43] I. Belyaev *et al.*, *Handling of the generation of primary events in Gauss, the LHCb simulation framework*, *J. Phys. Conf. Ser.* **331** (2011) 032047.
- [44] D. J. Lange, *The EvtGen particle decay simulation package*, *Nucl. Instrum. Meth.* **A462** (2001) 152.
- [45] N. Davidson, T. Przedzinski, and Z. Was, *PHOTOS interface in C++: Technical and physics documentation*, *Comput. Phys. Commun.* **199** (2016) 86, [arXiv:1011.0937](#).
- [46] Geant4 collaboration, J. Allison *et al.*, *Geant4 developments and applications*, *IEEE Trans. Nucl. Sci.* **53** (2006) 270; Geant4 collaboration, S. Agostinelli *et al.*, *Geant4: A simulation toolkit*, *Nucl. Instrum. Meth.* **A506** (2003) 250.

- [47] M. Clemencic *et al.*, *The LHCb simulation application, Gauss: Design, evolution and experience*, *J. Phys. Conf. Ser.* **331** (2011) 032023.
- [48] L. Anderlini *et al.*, *The PIDCalib package*, [LHCb-PUB-2016-021](#), 2016.
- [49] A. Poluektov, *Kernel density estimation of a multidimensional efficiency profile*, *JINST* **10** (2015) P02011, [arXiv:1411.5528](#).
- [50] R. Aaij *et al.*, *The LHCb trigger and its performance in 2011*, *JINST* **8** (2013) P04022, [arXiv:1211.3055](#).
- [51] V. V. Gligorov and M. Williams, *Efficient, reliable and fast high-level triggering using a bonsai boosted decision tree*, *JINST* **8** (2013) P02013, [arXiv:1210.6861](#).
- [52] T. Likhomanenko *et al.*, *LHCb topological trigger reoptimization*, *J. Phys. Conf. Ser.* **664** (2015) 082025, [arXiv:1510.00572](#).
- [53] T. Chen and C. Guestrin, *XGBoost: A scalable tree boosting system*, doi: [10.1145/2939672.2939785](#) [arXiv:1603.02754](#).
- [54] L. Breiman, J. H. Friedman, R. A. Olshen, and C. J. Stone, *Classification and regression trees*, Wadsworth international group, Belmont, California, USA, 1984.
- [55] G. Punzi, *Sensitivity of searches for new signals and its optimization*, eConf **C030908** (2003) MODT002, [arXiv:physics/0308063](#).
- [56] T. Skwarnicki, *A study of the radiative cascade transitions between the Upsilon-prime and Upsilon resonances*, PhD thesis, Institute of Nuclear Physics, Krakow, 1986, [DESY-F31-86-02](#).
- [57] ARGUS collaboration, H. Albrecht *et al.*, *Exclusive hadronic decays of B mesons*, *Z. Phys.* **C48** (1990) 543.
- [58] R. Barlow, *Event classification using weighting methods*, *J. Comput. Phys.* **72** (1987) 202.
- [59] M. Pivk and F. R. Le Diberder, *sPlot: A statistical tool to unfold data distributions*, *Nucl. Instrum. Meth.* **A555** (2005) 356, [arXiv:physics/0402083](#).
- [60] LHCb collaboration, R. Aaij *et al.*, *Precise measurement of the  $f_s/f_d$  ratio of fragmentation fractions and of  $B_s^0$  decay branching fractions*, *Phys. Rev.* **D104** (2021) 032005, [arXiv:2103.06810](#).
- [61] R. H. Dalitz, *On the analysis of  $\tau$ -meson data and the nature of the  $\tau$ -meson*, *Phil. Mag. Ser. 7* **44** (1953) 1068.
- [62] LHCb collaboration, R. Aaij *et al.*, *Amplitude analysis of  $B_s^0 \rightarrow K_S^0 K^\pm \pi^\mp$  decays*, *JHEP* **06** (2019) 114, [arXiv:1902.07955](#).
- [63] BaBar collaboration, B. Aubert *et al.*, *An amplitude analysis of the decay  $B^\pm \rightarrow \pi^\pm \pi^\pm \pi^\mp$* , *Phys. Rev.* **D72** (2005) 052002, [arXiv:hep-ex/0507025](#).

- [64] LHCb collaboration, R. Aaij *et al.*, *Measurement of the track reconstruction efficiency at LHCb*, *JINST* **10** (2015) P02007, [arXiv:1408.1251](#).
- [65] D. Martínez Santos and F. Dupertuis, *Mass distributions marginalized over per-event errors*, *Nucl. Instrum. Meth.* **A764** (2014) 150, [arXiv:1312.5000](#).
- [66] LHCb collaboration, R. Aaij *et al.*, *Observation of  $B_c^+ \rightarrow J/\psi D_s^+$  and  $B_c^+ \rightarrow J/\psi D_s^{*+}$  decays*, *Phys. Rev.* **D87** (2013) 112012, [arXiv:1304.4530](#).
- [67] R. Brun and F. Rademakers, *ROOT: An object oriented data analysis framework*, *Nucl. Instrum. Meth.* **A389** (1997) 81.

## LHCb collaboration

R. Aaij<sup>38</sup> , A.S.W. Abdelmotteleb<sup>57</sup> , C. Abellan Beteta<sup>51</sup> , F. Abudinén<sup>57</sup> ,  
 T. Ackernley<sup>61</sup> , A. A. Adefisoye<sup>69</sup> , B. Adeva<sup>47</sup> , M. Adinolfi<sup>55</sup> , P. Adlarson<sup>82</sup> ,  
 H. Afsharnia<sup>11</sup>, C. Agapopoulou<sup>14</sup> , C.A. Aidala<sup>83</sup> , Z. Ajaltouni<sup>11</sup>, S. Akar<sup>66</sup> ,  
 K. Akiba<sup>38</sup> , P. Albicocco<sup>28</sup> , J. Albrecht<sup>19,g</sup> , F. Alessio<sup>49</sup> , Z. Aliouche<sup>63</sup> ,  
 P. Alvarez Cartelle<sup>56</sup> , R. Amalric<sup>16</sup> , S. Amato<sup>3</sup> , J.L. Amey<sup>55</sup> , Y. Amhis<sup>14,49</sup> ,  
 L. An<sup>6</sup> , L. Anderlini<sup>27</sup> , M. Andersson<sup>51</sup> , A. Andreianov<sup>44</sup> , P. Andreola<sup>51</sup> ,  
 M. Andreotti<sup>26</sup> , D. Andreou<sup>69</sup> , A. Anelli<sup>31,p</sup> , D. Ao<sup>7</sup> , F. Archilli<sup>37,w</sup> ,  
 M. Argenton<sup>26</sup> , S. Arguedas Cuendis<sup>9,49</sup> , A. Artamonov<sup>44</sup> , M. Artuso<sup>69</sup> ,  
 E. Aslanides<sup>13</sup> , R. Ataíde Da Silva<sup>50</sup> , M. Atzeni<sup>65</sup> , B. Audurier<sup>12</sup> , D. Bacher<sup>64</sup> ,  
 I. Bachiller Perea<sup>10</sup> , S. Bachmann<sup>22</sup> , M. Bachmayer<sup>50</sup> , J.J. Back<sup>57</sup> ,  
 P. Baladron Rodriguez<sup>47</sup> , V. Balagura<sup>15</sup> , W. Baldini<sup>26</sup> , L. Balzani<sup>19</sup> , H. Bao<sup>7</sup> ,  
 J. Baptista de Souza Leite<sup>61</sup> , C. Barbero Pretel<sup>47,12</sup> , M. Barbetti<sup>27</sup> , I. R. Barbosa<sup>70</sup> ,  
 R.J. Barlow<sup>63,†</sup> , M. Barnyakov<sup>25</sup> , S. Barsuk<sup>14</sup> , W. Barter<sup>59</sup> , M. Bartolini<sup>56</sup> ,  
 J. Bartz<sup>69</sup> , J.M. Basels<sup>17</sup> , S. Bashir<sup>40</sup> , G. Bassi<sup>35,t</sup> , B. Batsukh<sup>5</sup> , P. B.  
 Battista<sup>14</sup> , A. Bay<sup>50</sup> , A. Beck<sup>57</sup> , M. Becker<sup>19</sup> , F. Bedeschi<sup>35</sup> , I.B. Bediaga<sup>2</sup> , N. A.  
 Behling<sup>19</sup> , S. Belin<sup>47</sup> , V. Bellee<sup>51</sup> , K. Belous<sup>44</sup> , I. Belov<sup>29</sup> , I. Belyaev<sup>36</sup> ,  
 G. Benane<sup>13</sup> , G. Bencivenni<sup>28</sup> , E. Ben-Haim<sup>16</sup> , A. Berezhnoy<sup>44</sup> , R. Bernet<sup>51</sup> ,  
 S. Bernet Andres<sup>46</sup> , E. Bertholet<sup>16</sup> , A. Bertolin<sup>33</sup> , C. Betancourt<sup>51</sup> , F. Betti<sup>59</sup> , J.  
 Bex<sup>56</sup> , Ia. Bezshyiko<sup>51</sup> , J. Bhom<sup>41</sup> , M.S. Bieker<sup>19</sup> , N.V. Biesuz<sup>26</sup> , P. Billoir<sup>16</sup> ,  
 A. Biolchini<sup>38</sup> , M. Birch<sup>62</sup> , F.C.R. Bishop<sup>10</sup> , A. Bitadze<sup>63</sup> , A. Bizzeti<sup>27,q</sup> ,  
 T. Blake<sup>57</sup> , F. Blanc<sup>50</sup> , J.E. Blank<sup>19</sup> , S. Blusk<sup>69</sup> , V. Bocharnikov<sup>44</sup> ,  
 J.A. Boelhauve<sup>19</sup> , O. Boente Garcia<sup>15</sup> , T. Boettcher<sup>66</sup> , A. Bohare<sup>59</sup> ,  
 A. Boldyrev<sup>44</sup> , C. Bolognani<sup>79</sup> , R. Bolzonella<sup>26,m</sup> , N. Bondar<sup>44</sup> , A. Bordelius<sup>49</sup> ,  
 F. Borgato<sup>33,r</sup> , S. Borghi<sup>63</sup> , M. Borsato<sup>31,p</sup> , J.T. Borsuk<sup>41</sup> , S.A. Bouchiba<sup>50</sup> , M.  
 Bovill<sup>64</sup> , T.J.V. Bowcock<sup>61</sup> , A. Boyer<sup>49</sup> , C. Bozzi<sup>26</sup> , A. Brea Rodriguez<sup>50</sup> ,  
 N. Breer<sup>19</sup> , J. Brodzicka<sup>41</sup> , A. Brossa Gonzalo<sup>57,47,45,†</sup> , J. Brown<sup>61</sup> , D. Brundu<sup>32</sup> ,  
 E. Buchanan<sup>59</sup> , A. Buonaura<sup>51</sup> , L. Buonincontri<sup>33,r</sup> , A.T. Burke<sup>63</sup> , C. Burr<sup>49</sup> ,  
 J.S. Butter<sup>56</sup> , J. Buytaert<sup>49</sup> , W. Byczynski<sup>49</sup> , S. Cadeddu<sup>32</sup> , H. Cai<sup>74</sup> ,  
 A. Caillet<sup>16</sup> , R. Calabrese<sup>26,m</sup> , S. Calderon Ramirez<sup>9</sup> , L. Calefice<sup>45</sup> , S. Cali<sup>28</sup> ,  
 M. Calvi<sup>31,p</sup> , M. Calvo Gomez<sup>46</sup> , P. Camargo Magalhaes<sup>2,a</sup> , J. I. Cambon Bouzas<sup>47</sup> ,  
 P. Campana<sup>28</sup> , D.H. Campora Perez<sup>79</sup> , A.F. Campoverde Quezada<sup>7</sup> , S. Capelli<sup>31</sup> ,  
 L. Capriotti<sup>26</sup> , R. Caravaca-Mora<sup>9</sup> , A. Carbone<sup>25,k</sup> , L. Carcedo Salgado<sup>47</sup> ,  
 R. Cardinale<sup>29,n</sup> , A. Cardini<sup>32</sup> , P. Carniti<sup>31,p</sup> , L. Carus<sup>22</sup> , A. Casais Vidal<sup>65</sup> ,  
 R. Caspary<sup>22</sup> , G. Casse<sup>61</sup> , M. Cattaneo<sup>49</sup> , G. Cavallero<sup>26,49</sup> , V. Cavallini<sup>26,m</sup> ,  
 S. Celani<sup>22</sup> , D. Cervenkov<sup>64</sup> , S. Cesare<sup>30,o</sup> , A.J. Chadwick<sup>61</sup> , I. Chahrour<sup>83</sup> ,  
 M. Charles<sup>16</sup> , Ph. Charpentier<sup>49</sup> , E. Chatzianagnostou<sup>38</sup> , M. Chefdeville<sup>10</sup> ,  
 C. Chen<sup>13</sup> , S. Chen<sup>5</sup> , Z. Chen<sup>7</sup> , A. Chernov<sup>41</sup> , S. Chernyshenko<sup>53</sup> , X.  
 Chiotopoulos<sup>79</sup> , V. Chobanova<sup>81</sup> , S. Cholak<sup>50</sup> , M. Chrzaszcz<sup>41</sup> , A. Chubykin<sup>44</sup> ,  
 V. Chulikov<sup>44</sup> , P. Ciambone<sup>28</sup> , X. Cid Vidal<sup>47</sup> , G. Ciezarek<sup>49</sup> , P. Cifra<sup>49</sup> ,  
 P.E.L. Clarke<sup>59</sup> , M. Clemencic<sup>49</sup> , H.V. Cliff<sup>56</sup> , J. Closier<sup>49</sup> , C. Cocha Toapaxi<sup>22</sup> ,  
 V. Coco<sup>49</sup> , J. Cogan<sup>13</sup> , E. Cogneras<sup>11</sup> , L. Cojocariu<sup>43</sup> , P. Collins<sup>49</sup> ,  
 T. Colombo<sup>49</sup> , M. Colonna<sup>19</sup> , A. Comerma-Montells<sup>45</sup> , L. Congedo<sup>24</sup> , A. Contu<sup>32</sup> ,  
 N. Cooke<sup>60</sup> , I. Corredoira<sup>47</sup> , A. Correia<sup>16</sup> , G. Corti<sup>49</sup> , J. Cottee Meldrum<sup>55</sup> ,  
 B. Couturier<sup>49</sup> , D.C. Craik<sup>51</sup> , M. Cruz Torres<sup>2,h</sup> , E. Curras Rivera<sup>50</sup> , R. Currie<sup>59</sup> ,  
 C.L. Da Silva<sup>68</sup> , S. Dadabaev<sup>44</sup> , L. Dai<sup>71</sup> , X. Dai<sup>6</sup> , E. Dall'Occo<sup>49</sup> , J. Dalseno<sup>47</sup> ,  
 C. D'Ambrosio<sup>49</sup> , J. Daniel<sup>11</sup> , A. Danilina<sup>44</sup> , P. d'Argent<sup>24</sup> , A. Davidson<sup>57</sup> ,  
 J.E. Davies<sup>63</sup> , A. Davis<sup>63</sup> , O. De Aguiar Francisco<sup>63</sup> , C. De Angelis<sup>32,l</sup> ,  
 F. De Benedetti<sup>49</sup> , J. de Boer<sup>38</sup> , K. De Bruyn<sup>78</sup> , S. De Capua<sup>63</sup> , M. De Cian<sup>22,49</sup> ,

U. De Freitas Carneiro Da Graca<sup>2,b</sup> , E. De Lucia<sup>28</sup> , J.M. De Miranda<sup>2</sup> , L. De Paula<sup>3</sup> ,  
 M. De Serio<sup>24,i</sup> , P. De Simone<sup>28</sup> , F. De Vellis<sup>19</sup> , J.A. de Vries<sup>79</sup> , F. Debernardis<sup>24</sup> ,  
 D. Decamp<sup>10</sup> , V. Dedu<sup>13</sup> , S. Dekkers<sup>1</sup> , L. Del Buono<sup>16</sup> , B. Delaney<sup>65</sup> ,  
 H.-P. Dembinski<sup>19</sup> , J. Deng<sup>8</sup> , V. Denysenko<sup>51</sup> , O. Deschamps<sup>11</sup> , F. Dettori<sup>32,l</sup> ,  
 B. Dey<sup>77</sup> , P. Di Nezza<sup>28</sup> , I. Diachkov<sup>44</sup> , S. Didenko<sup>44</sup> , S. Ding<sup>69</sup> , L. Dittmann<sup>22</sup> ,  
 V. Dobishuk<sup>53</sup> , A. D. Docheva<sup>60</sup> , C. Dong<sup>4,c</sup> , A.M. Donohoe<sup>23</sup> , F. Dordei<sup>32</sup> ,  
 A.C. dos Reis<sup>2</sup> , A. D. Dowling<sup>69</sup> , W. Duan<sup>72</sup> , P. Duda<sup>80</sup> , M.W. Dudek<sup>41</sup> ,  
 L. Dufour<sup>49</sup> , V. Duk<sup>34</sup> , P. Durante<sup>49</sup> , M. M. Duras<sup>80</sup> , J.M. Durham<sup>68</sup> , O. D.  
 Durmus<sup>77</sup> , A. Dziurda<sup>41</sup> , A. Dzyuba<sup>44</sup> , S. Easo<sup>58</sup> , E. Eckstein<sup>18</sup> , U. Egede<sup>1</sup> ,  
 A. Egorychev<sup>44</sup> , V. Egorychev<sup>44</sup> , S. Eisenhardt<sup>59</sup> , E. Ejopu<sup>63</sup> , L. Eklund<sup>82</sup> ,  
 M. Elashri<sup>66</sup> , J. Ellbracht<sup>19</sup> , S. Ely<sup>62</sup> , A. Ene<sup>43</sup> , E. Epple<sup>66</sup> , J. Eschle<sup>69</sup> ,  
 S. Esen<sup>22</sup> , T. Evans<sup>63</sup> , F. Fabiano<sup>32,l</sup> , L.N. Falcao<sup>2</sup> , Y. Fan<sup>7</sup> , B. Fang<sup>7</sup> ,  
 L. Fantini<sup>34,s,49</sup> , M. Faria<sup>50</sup> , K. Farmer<sup>59</sup> , D. Fazzini<sup>31,p</sup> , L. Felkowski<sup>80</sup> ,  
 M. Feng<sup>5,7</sup> , M. Feo<sup>19,49</sup> , A. Fernandez Casani<sup>48</sup> , M. Fernandez Gomez<sup>47</sup> ,  
 A.D. Fernez<sup>67</sup> , F. Ferrari<sup>25,k</sup> , F. Ferreira Rodrigues<sup>3</sup> , M. Ferrillo<sup>51</sup> ,  
 M. Ferro-Luzzi<sup>49</sup> , S. Filippov<sup>44</sup> , R.A. Fini<sup>24</sup> , M. Fiorini<sup>26,m</sup> , M. Firlej<sup>40</sup> ,  
 K.L. Fischer<sup>64</sup> , D.S. Fitzgerald<sup>83</sup> , C. Fitzpatrick<sup>63</sup> , T. Fiutowski<sup>40</sup> , F. Fleuret<sup>15</sup> ,  
 M. Fontana<sup>25</sup> , L. A. Foreman<sup>63</sup> , R. Forty<sup>49</sup> , D. Foulds-Holt<sup>56</sup> , V. Franco Lima<sup>3</sup> ,  
 M. Franco Sevilla<sup>67</sup> , M. Frank<sup>49</sup> , E. Franzoso<sup>26,m</sup> , G. Frau<sup>63</sup> , C. Frei<sup>49</sup> ,  
 D.A. Friday<sup>63</sup> , J. Fu<sup>7</sup> , Q. Führung<sup>19,g,56</sup> , Y. Fujii<sup>1</sup> , T. Fulghesu<sup>16</sup> , E. Gabriel<sup>38</sup> ,  
 G. Galati<sup>24</sup> , M.D. Galati<sup>38</sup> , A. Gallas Torreira<sup>47</sup> , D. Galli<sup>25,k</sup> , S. Gambetta<sup>59</sup> ,  
 M. Gandelman<sup>3</sup> , P. Gandini<sup>30</sup> , B. Ganie<sup>63</sup> , H. Gao<sup>7</sup> , R. Gao<sup>64</sup> , T.Q. Gao<sup>56</sup> ,  
 Y. Gao<sup>8</sup> , Y. Gao<sup>6</sup> , Y. Gao<sup>8</sup> , L.M. Garcia Martin<sup>50</sup> , P. Garcia Moreno<sup>45</sup> ,  
 J. García Pardiñas<sup>49</sup> , K. G. Garg<sup>8</sup> , L. Garrido<sup>45</sup> , C. Gaspar<sup>49</sup> , R.E. Geertsema<sup>38</sup> ,  
 L.L. Gerken<sup>19</sup> , E. Gersabeck<sup>63</sup> , M. Gersabeck<sup>20</sup> , T. Gershon<sup>57</sup> , S. Ghizzo<sup>29,n</sup> ,  
 Z. Ghorbanimoghaddam<sup>55</sup> , L. Giambastiani<sup>33,r</sup> , F. I. Giasemis<sup>16,f</sup> , V. Gibson<sup>56</sup> ,  
 H.K. Giemza<sup>42</sup> , A.L. Gilman<sup>64</sup> , M. Giovannetti<sup>28</sup> , A. Gioventù<sup>45</sup> , L. Girardey<sup>63,58</sup> ,  
 P. Gironella Gironell<sup>45</sup> , C. Giugliano<sup>26,m</sup> , M.A. Giza<sup>41</sup> , E.L. Gkoukousis<sup>62</sup> ,  
 F.C. Glaser<sup>14,22</sup> , V.V. Gligorov<sup>16,49</sup> , C. Göbel<sup>70</sup> , E. Golobardes<sup>46</sup> , D. Golubkov<sup>44</sup> ,  
 A. Golutvin<sup>62,49,44</sup> , S. Gomez Fernandez<sup>45</sup> , F. Goncalves Abrantes<sup>64</sup> , M. Goncerz<sup>41</sup> ,  
 G. Gong<sup>4,c</sup> , J. A. Gooding<sup>19</sup> , I.V. Gorelov<sup>44</sup> , C. Gotti<sup>31</sup> , J.P. Grabowski<sup>18</sup> ,  
 T. Grammatico<sup>16</sup> , L.A. Granado Cardoso<sup>49</sup> , E. Graugés<sup>45</sup> , E. Graverini<sup>50,u</sup> ,  
 L. Gazette<sup>57</sup> , G. Graziani<sup>27</sup> , A. T. Grecu<sup>43</sup> , L.M. Greeven<sup>38</sup> , N.A. Grieser<sup>66</sup> ,  
 L. Grillo<sup>60</sup> , S. Gromov<sup>44</sup> , C. Gu<sup>15</sup> , M. Guarise<sup>26</sup> , L. Guerry<sup>11</sup> , M. Guittiere<sup>14</sup> ,  
 V. Guliaeva<sup>44</sup> , P. A. Günther<sup>22</sup> , A.-K. Guseinov<sup>50</sup> , E. Gushchin<sup>44</sup> , Y. Guz<sup>6,49,44</sup> ,  
 T. Gys<sup>49</sup> , K. Habermann<sup>18</sup> , T. Hadavizadeh<sup>1</sup> , C. Hadjivasiliou<sup>67</sup> , G. Haefeli<sup>50</sup> ,  
 C. Haen<sup>49</sup> , J. Haimberger<sup>49</sup> , M. Hajheidari<sup>49</sup> , G. Hallett<sup>57</sup> , M.M. Halvorsen<sup>49</sup> ,  
 P.M. Hamilton<sup>67</sup> , J. Hammerich<sup>61</sup> , Q. Han<sup>8</sup> , X. Han<sup>22,49</sup> ,  
 S. Hansmann-Menzemer<sup>22</sup> , L. Hao<sup>7</sup> , N. Harnew<sup>64</sup> , M. Hartmann<sup>14</sup> , S. Hashmi<sup>40</sup> ,  
 J. He<sup>7,d</sup> , F. Hemmer<sup>49</sup> , C. Henderson<sup>66</sup> , R.D.L. Henderson<sup>1,57</sup> , A.M. Hennequin<sup>49</sup> ,  
 K. Hennessy<sup>61</sup> , L. Henry<sup>50</sup> , J. Herd<sup>62</sup> , P. Herrero Gascon<sup>22</sup> , J. Heuel<sup>17</sup> ,  
 A. Hicheur<sup>3</sup> , G. Hijano Mendizabal<sup>51</sup> , D. Hill<sup>50</sup> , J. Horswill<sup>63</sup> , R. Hou<sup>8</sup> ,  
 Y. Hou<sup>11</sup> , N. Howarth<sup>61</sup> , J. Hu<sup>72</sup> , W. Hu<sup>6</sup> , X. Hu<sup>4,c</sup> , W. Huang<sup>7</sup> ,  
 W. Hulsbergen<sup>38</sup> , R.J. Hunter<sup>57</sup> , M. Hushchyn<sup>44</sup> , D. Hutchcroft<sup>61</sup> , M. Idzik<sup>40</sup> ,  
 D. Ilin<sup>44</sup> , P. Ilten<sup>66</sup> , A. Inglessi<sup>44</sup> , A. Iniukhin<sup>44</sup> , A. Ishteev<sup>44</sup> , K. Ivshin<sup>44</sup> ,  
 R. Jacobsson<sup>49</sup> , H. Jage<sup>17</sup> , S.J. Jaimes Elles<sup>48,75</sup> , S. Jakobsen<sup>49</sup> , E. Jans<sup>38</sup> ,  
 B.K. Jashal<sup>48</sup> , A. Jawahery<sup>67,49</sup> , V. Jevtic<sup>19</sup> , E. Jiang<sup>67</sup> , X. Jiang<sup>5,7</sup> , Y. Jiang<sup>7</sup> ,  
 Y. J. Jiang<sup>6</sup> , M. John<sup>64</sup> , A. John Rubesh Rajan<sup>23</sup> , D. Johnson<sup>54</sup> , C.R. Jones<sup>56</sup> ,  
 T.P. Jones<sup>57</sup> , S. Joshi<sup>42</sup> , B. Jost<sup>49</sup> , J. Juan Castella<sup>56</sup> , N. Jurik<sup>49</sup> , I. Juszcak<sup>41</sup> ,  
 D. Kaminaris<sup>50</sup> , S. Kandybei<sup>52</sup> , M. Kane<sup>59</sup> , Y. Kang<sup>4,c</sup> , C. Kar<sup>11</sup> ,

M. Karacson<sup>49</sup> , D. Karpenkov<sup>44</sup> , A. Kauniskangas<sup>50</sup> , J.W. Kautz<sup>66</sup> ,  
M.K. Kazanecki<sup>41</sup> , F. Keizer<sup>49</sup> , M. Kenzie<sup>56</sup> , T. Ketel<sup>38</sup> , B. Khanji<sup>69</sup> ,  
A. Kharisova<sup>44</sup> , S. Kholodenko<sup>35,49</sup> , G. Khreich<sup>14</sup> , T. Kirn<sup>17</sup> , V.S. Kirsebom<sup>31,p</sup> ,  
O. Kitouni<sup>65</sup> , S. Klaver<sup>39</sup> , N. Kleijne<sup>35,t</sup> , K. Klimaszewski<sup>42</sup> , M.R. Kmiec<sup>42</sup> ,  
S. Koliiev<sup>53</sup> , L. Kolk<sup>19</sup> , A. Konoplyannikov<sup>44</sup> , P. Kopciwicz<sup>40,49</sup> , P. Koppenburg<sup>38</sup> ,  
M. Korolev<sup>44</sup> , I. Kostiuk<sup>38</sup> , O. Kot<sup>53</sup> , S. Kotriakhova , A. Kozachuk<sup>44</sup> ,  
P. Kravchenko<sup>44</sup> , L. Kravchuk<sup>44</sup> , M. Kreps<sup>57</sup> , P. Krovovny<sup>44</sup> , W. Krupa<sup>69</sup> ,  
W. Krzemien<sup>42</sup> , O. Kshyvanskyi<sup>53</sup> , S. Kubis<sup>80</sup> , M. Kucharczyk<sup>41</sup> , V. Kudryavtsev<sup>44</sup> ,  
E. Kulikova<sup>44</sup> , A. Kupsc<sup>82</sup> , B. Kutsenko<sup>13</sup> , D. Lacarrere<sup>49</sup> , P. Laguarda Gonzalez<sup>45</sup> ,  
A. Lai<sup>32</sup> , A. Lampis<sup>32</sup> , D. Lancierini<sup>56</sup> , C. Landesa Gomez<sup>47</sup> , J.J. Lane<sup>1</sup> ,  
R. Lane<sup>55</sup> , G. Lanfranchi<sup>28</sup> , C. Langenbruch<sup>22</sup> , J. Langer<sup>19</sup> , O. Lantwin<sup>44</sup> ,  
T. Latham<sup>57</sup> , F. Lazzari<sup>35,u</sup> , C. Lazzeroni<sup>54</sup> , R. Le Gac<sup>13</sup> , H. Lee<sup>61</sup> ,  
R. Lefevre<sup>11</sup> , A. Leflat<sup>44</sup> , S. Legotin<sup>44</sup> , M. Lehuraux<sup>57</sup> , E. Lemos Cid<sup>49</sup> ,  
O. Leroy<sup>13</sup> , T. Lesiak<sup>41</sup> , E. D. Lesser<sup>49</sup> , B. Leverington<sup>22</sup> , A. Li<sup>4,c</sup> , C. Li<sup>13</sup> ,  
H. Li<sup>72</sup> , K. Li<sup>8</sup> , L. Li<sup>63</sup> , M. Li<sup>8</sup> , P. Li<sup>7</sup> , P.-R. Li<sup>73</sup> , Q. Li<sup>5,7</sup> , S. Li<sup>8</sup> ,  
T. Li<sup>5,e</sup> , T. Li<sup>72</sup> , Y. Li<sup>8</sup> , Y. Li<sup>5</sup> , Z. Lian<sup>4,c</sup> , X. Liang<sup>69</sup> , S. Libralon<sup>48</sup> ,  
C. Lin<sup>7</sup> , T. Lin<sup>58</sup> , R. Lindner<sup>49</sup> , V. Lisovskyi<sup>50</sup> , R. Litvinov<sup>32,49</sup> , F. L. Liu<sup>1</sup> ,  
G. Liu<sup>72</sup> , K. Liu<sup>73</sup> , S. Liu<sup>5,7</sup> , W. Liu<sup>8</sup> , Y. Liu<sup>59</sup> , Y. Liu<sup>73</sup> , Y. L. Liu<sup>62</sup> ,  
A. Lobo Salvia<sup>45</sup> , A. Loi<sup>32</sup> , J. Lomba Castro<sup>47</sup> , T. Long<sup>56</sup> , J.H. Lopes<sup>3</sup> ,  
A. Lopez Huertas<sup>45</sup> , S. López Soliño<sup>47</sup> , Q. Lu<sup>15</sup> , C. Lucarelli<sup>27</sup> , D. Lucchesi<sup>33,r</sup> ,  
M. Lucio Martinez<sup>79</sup> , V. Lukashenko<sup>38,53</sup> , Y. Luo<sup>6</sup> , A. Lupato<sup>33,j</sup> , E. Luppi<sup>26,m</sup> ,  
K. Lynch<sup>23</sup> , X.-R. Lyu<sup>7</sup> , G. M. Ma<sup>4,c</sup> , S. Maccolini<sup>19</sup> , F. Machefert<sup>14</sup> ,  
F. Maciuc<sup>43</sup> , B. Mack<sup>69</sup> , I. Mackay<sup>64</sup> , L. M. Mackey<sup>69</sup> , L.R. Madhan Mohan<sup>56</sup> , M.  
J. Madurai<sup>54</sup> , A. Maevskiy<sup>44</sup> , D. Magdalinski<sup>38</sup> , D. Maisuzenko<sup>44</sup> , M.W. Majewski<sup>40</sup> ,  
J.J. Malczewski<sup>41</sup> , S. Malde<sup>64</sup> , L. Malentacca<sup>49</sup> , A. Malinin<sup>44</sup> , T. Maltsev<sup>44</sup> ,  
G. Manca<sup>32,l</sup> , G. Mancinelli<sup>13</sup> , C. Mancuso<sup>30,14,o</sup> , R. Manera Escalero<sup>45</sup> , F. M.  
Manganella<sup>37</sup> , D. Manuzzi<sup>25</sup> , D. Marangotto<sup>30,o</sup> , J.F. Marchand<sup>10</sup> ,  
R. Marchevski<sup>50</sup> , U. Marconi<sup>25</sup> , E. Mariani<sup>16</sup> , S. Mariani<sup>49</sup> , C. Marin Benito<sup>45,49</sup> ,  
J. Marks<sup>22</sup> , A.M. Marshall<sup>55</sup> , L. Martel<sup>64</sup> , G. Martelli<sup>34,s</sup> , G. Martellotti<sup>36</sup> ,  
L. Martinazzoli<sup>49</sup> , M. Martinelli<sup>31,p</sup> , D. Martinez Santos<sup>47</sup> , F. Martinez Vidal<sup>48</sup> ,  
A. Massafferri<sup>2</sup> , R. Matev<sup>49</sup> , A. Mathad<sup>49</sup> , V. Matiunin<sup>44</sup> , C. Matteuzzi<sup>69</sup> ,  
K.R. Mattioli<sup>15</sup> , A. Mauri<sup>62</sup> , E. Maurice<sup>15</sup> , J. Mauricio<sup>45</sup> , P. Mayencourt<sup>50</sup> ,  
J. Mazorra de Cos<sup>48</sup> , M. Mazurek<sup>42</sup> , M. McCann<sup>62</sup> , L. McConnell<sup>23</sup> ,  
T.H. McGrath<sup>63</sup> , N.T. McHugh<sup>60</sup> , A. McNab<sup>63</sup> , R. McNulty<sup>23</sup> , B. Meadows<sup>66</sup> ,  
G. Meier<sup>19</sup> , D. Melnychuk<sup>42</sup> , F. M. Meng<sup>4,c</sup> , M. Merk<sup>38,79</sup> , A. Merli<sup>50</sup> ,  
L. Meyer Garcia<sup>67</sup> , D. Miao<sup>5,7</sup> , H. Miao<sup>7</sup> , M. Mikhasenko<sup>76</sup> , D.A. Milanes<sup>75</sup> ,  
A. Minotti<sup>31,p</sup> , E. Minucci<sup>69</sup> , T. Miralles<sup>11</sup> , B. Mitreska<sup>19</sup> , D.S. Mitzel<sup>19</sup> ,  
A. Modak<sup>58</sup> , R.A. Mohammed<sup>64</sup> , R.D. Moise<sup>17</sup> , S. Mokhnenko<sup>44</sup> , E.  
F. Molina Cardenas<sup>83</sup> , T. Mombächer<sup>49</sup> , M. Monk<sup>57,1</sup> , S. Monteil<sup>11</sup> ,  
A. Morcillo Gomez<sup>47</sup> , G. Morello<sup>28</sup> , M.J. Morello<sup>35,t</sup> , M.P. Morgenthaler<sup>22</sup> ,  
J. Moron<sup>40</sup> , A.B. Morris<sup>49</sup> , A.G. Morris<sup>13</sup> , R. Mountain<sup>69</sup> , H. Mu<sup>4,c</sup> , Z. Mu<sup>6</sup> ,  
E. Muhammad<sup>57</sup> , F. Muheim<sup>59</sup> , M. Mulder<sup>78</sup> , K. Müller<sup>51</sup> , F. Muñoz-Rojas<sup>9</sup> ,  
R. Murta<sup>62</sup> , P. Naik<sup>61</sup> , T. Nakada<sup>50</sup> , R. Nandakumar<sup>58</sup> , T. Namut<sup>49</sup> , I. Nasteva<sup>3</sup> ,  
M. Needham<sup>59</sup> , N. Neri<sup>30,o</sup> , S. Neubert<sup>18</sup> , N. Neufeld<sup>49</sup> , P. Neustroev<sup>44</sup> ,  
J. Nicolini<sup>19,14</sup> , D. Nicotra<sup>79</sup> , E.M. Niel<sup>50</sup> , N. Nikitin<sup>44</sup> , Q. Niu<sup>73</sup> , P. Nogarolli<sup>3</sup> ,  
P. Nogga<sup>18</sup> , C. Normand<sup>55</sup> , J. Novoa Fernandez<sup>47</sup> , G. Nowak<sup>66</sup> , C. Nunez<sup>83</sup> , H. N.  
Nur<sup>60</sup> , A. Oblakowska-Mucha<sup>40</sup> , V. Obratsov<sup>44</sup> , T. Oeser<sup>17</sup> , S. Okamura<sup>26,m</sup> ,  
A. Okhotnikov<sup>44</sup> , O. Okhrimenko<sup>53</sup> , R. Oldeman<sup>32,l</sup> , F. Oliva<sup>59</sup> , M. Olocco<sup>19</sup> ,  
C.J.G. Onderwater<sup>79</sup> , R.H. O'Neil<sup>59</sup> , J.S. Ordonez Soto<sup>75</sup> , D. Osthues<sup>19</sup> ,  
J.M. Otalora Goicochea<sup>3</sup> , P. Owen<sup>51</sup> , A. Oyanguren<sup>48</sup> , O. Ozcelik<sup>59</sup> , F. Paciolla<sup>35,x</sup> 

A. Padee<sup>42</sup> , K.O. Padeken<sup>18</sup> , B. Pagare<sup>57</sup> , P.R. Pais<sup>22</sup> , T. Pajero<sup>49</sup> , A. Palano<sup>24</sup> ,  
 M. Palutan<sup>28</sup> , G. Panshin<sup>44</sup> , L. Paolucci<sup>57</sup> , A. Papanestis<sup>58,49</sup> , M. Pappagallo<sup>24,i</sup> ,  
 L.L. Pappalardo<sup>26,m</sup> , C. Pappenheimer<sup>66</sup> , C. Parkes<sup>63</sup> , B. Passalacqua<sup>26,m</sup> ,  
 G. Passaleva<sup>27</sup> , D. Passaro<sup>35,t</sup> , A. Pastore<sup>24</sup> , M. Patel<sup>62</sup> , J. Patoc<sup>64</sup> ,  
 C. Patrignani<sup>25,k</sup> , A. Paul<sup>69</sup> , C.J. Pawley<sup>79</sup> , A. Pellegrino<sup>38</sup> , J. Peng<sup>5,7</sup> ,  
 M. Pepe Altarelli<sup>28</sup> , S. Perazzini<sup>25</sup> , D. Pereima<sup>44</sup> , H. Pereira Da Costa<sup>68</sup> ,  
 A. Pereiro Castro<sup>47</sup> , P. Perret<sup>11</sup> , A. Perro<sup>49,13</sup> , K. Petridis<sup>55</sup> , A. Petrolini<sup>29,n</sup> , J. P.  
 Pfaller<sup>66</sup> , H. Pham<sup>69</sup> , L. Pica<sup>35,t</sup> , M. Piccini<sup>34</sup> , L. Piccolo<sup>32</sup> , B. Pietrzyk<sup>10</sup> ,  
 G. Pietrzyk<sup>14</sup> , D. Pinci<sup>36</sup> , F. Pisani<sup>49</sup> , M. Pizzichemi<sup>31,p,49</sup> , V. M. Placinta<sup>43</sup> ,  
 M. Plo Casasus<sup>47</sup> , T. Poeschl<sup>49</sup> , F. Polci<sup>16,49</sup> , M. Poli Lener<sup>28</sup> , A. Poluektov<sup>13</sup> ,  
 N. Polukhina<sup>44</sup> , I. Polyakov<sup>44</sup> , E. Polcarpo<sup>3</sup> , S. Ponce<sup>49</sup> , D. Popov<sup>7</sup> ,  
 S. Poslavskii<sup>44</sup> , K. Prasanth<sup>59</sup> , C. Prouve<sup>47</sup> , D. Provenzano<sup>32,l</sup> , V. Pugatch<sup>53</sup> ,  
 G. Punzi<sup>35,u</sup> , S. Qasim<sup>51</sup> , Q. Qian<sup>6</sup> , W. Qian<sup>7</sup> , N. Qin<sup>4,c</sup> , S. Qu<sup>4,c</sup> ,  
 R. Quagliani<sup>49</sup> , R.I. Rabadan Trejo<sup>57</sup> , J.H. Rademacker<sup>55</sup> , M. Rama<sup>35</sup> , M.  
 Ramírez García<sup>83</sup> , V. Ramos De Oliveira<sup>70</sup> , M. Ramos Pernas<sup>57</sup> , M.S. Rangel<sup>3</sup> ,  
 F. Ratnikov<sup>44</sup> , G. Raven<sup>39</sup> , M. Rebollo De Miguel<sup>48</sup> , F. Redi<sup>30,j</sup> , J. Reich<sup>55</sup> ,  
 F. Reiss<sup>63</sup> , Z. Ren<sup>7</sup> , P.K. Resmi<sup>64</sup> , R. Ribatti<sup>50</sup> , G. Ricart<sup>15,12</sup> , D. Riccardi<sup>35,t</sup> ,  
 S. Ricciardi<sup>58</sup> , K. Richardson<sup>65</sup> , M. Richardson-Slipper<sup>59</sup> , K. Rinnert<sup>61</sup> ,  
 P. Robbe<sup>14,49</sup> , G. Robertson<sup>60</sup> , E. Rodrigues<sup>61</sup> , E. Rodriguez Fernandez<sup>47</sup> ,  
 J.A. Rodriguez Lopez<sup>75</sup> , E. Rodriguez Rodriguez<sup>47</sup> , J. Roensch<sup>19</sup> , A. Rogachev<sup>44</sup> ,  
 A. Rogovskiy<sup>58</sup> , D.L. Rolf<sup>49</sup> , P. Roloff<sup>49</sup> , V. Romanovskiy<sup>66</sup> , A. Romero Vidal<sup>47</sup> ,  
 G. Romolini<sup>26</sup> , F. Ronchetti<sup>50</sup> , T. Rong<sup>6</sup> , M. Rotondo<sup>28</sup> , S. R. Roy<sup>22</sup> ,  
 M.S. Rudolph<sup>69</sup> , M. Ruiz Diaz<sup>22</sup> , R.A. Ruiz Fernandez<sup>47</sup> , J. Ruiz Vidal<sup>82,aa</sup> ,  
 A. Ryzhikov<sup>44</sup> , J. Ryzka<sup>40</sup> , J. J. Saavedra-Arias<sup>9</sup> , J.J. Saborido Silva<sup>47</sup> , R. Sadek<sup>15</sup> ,  
 N. Sagidova<sup>44</sup> , D. Sahoo<sup>77</sup> , N. Sahoo<sup>54</sup> , B. Saitta<sup>32,l</sup> , M. Salomoni<sup>31,49,p</sup> ,  
 I. Sanderswood<sup>48</sup> , R. Santacesaria<sup>36</sup> , C. Santamarina Rios<sup>47</sup> , M. Santimaria<sup>28,49</sup> ,  
 L. Santoro<sup>2</sup> , E. Santovetti<sup>37</sup> , A. Saputi<sup>26,49</sup> , D. Saranin<sup>44</sup> , A. Sarnatskiy<sup>78</sup> ,  
 G. Sarpis<sup>59</sup> , M. Sarpis<sup>63</sup> , C. Satriano<sup>36,v</sup> , A. Satta<sup>37</sup> , M. Saur<sup>6</sup> , D. Savrina<sup>44</sup> ,  
 H. Sazak<sup>17</sup> , F. Sborzacchi<sup>49,28</sup> , L.G. Scantlebury Smead<sup>64</sup> , A. Scarabotto<sup>19</sup> ,  
 S. Schael<sup>17</sup> , S. Scherl<sup>61</sup> , M. Schiller<sup>60</sup> , H. Schindler<sup>49</sup> , M. Schmelling<sup>21</sup> ,  
 B. Schmidt<sup>49</sup> , S. Schmitt<sup>17</sup> , H. Schmitz<sup>18</sup> , O. Schneider<sup>50</sup> , A. Schopper<sup>49</sup> ,  
 N. Schulte<sup>19</sup> , S. Schulte<sup>50</sup> , M.H. Schune<sup>14</sup> , R. Schwemmer<sup>49</sup> , G. Schwering<sup>17</sup> ,  
 B. Sciascia<sup>28</sup> , A. Sciuccati<sup>49</sup> , S. Sellam<sup>47</sup> , A. Semennikov<sup>44</sup> , T. Senger<sup>51</sup> ,  
 M. Senghi Soares<sup>39</sup> , A. Sergi<sup>29,n</sup> , N. Serra<sup>51</sup> , L. Sestini<sup>33</sup> , A. Seuthe<sup>19</sup> ,  
 Y. Shang<sup>6</sup> , D.M. Shangase<sup>83</sup> , M. Shapkin<sup>44</sup> , R. S. Sharma<sup>69</sup> , I. Shchemerov<sup>44</sup> ,  
 L. Shchutska<sup>50</sup> , T. Shears<sup>61</sup> , L. Shekhtman<sup>44</sup> , Z. Shen<sup>6</sup> , S. Sheng<sup>5,7</sup> ,  
 V. Shevchenko<sup>44</sup> , B. Shi<sup>7</sup> , Q. Shi<sup>7</sup> , Y. Shimizu<sup>14</sup> , E. Shmanin<sup>25</sup> , R. Shorkin<sup>44</sup> ,  
 J.D. Shupperd<sup>69</sup> , R. Silva Coutinho<sup>69</sup> , G. Simi<sup>33,r</sup> , S. Simone<sup>24,i</sup> , N. Skidmore<sup>57</sup> ,  
 T. Skwarnicki<sup>69</sup> , M.W. Slater<sup>54</sup> , J.C. Smallwood<sup>64</sup> , E. Smith<sup>65</sup> , K. Smith<sup>68</sup> ,  
 M. Smith<sup>62</sup> , A. Snoch<sup>38</sup> , L. Soares Lavra<sup>59</sup> , M.D. Sokoloff<sup>66</sup> , F.J.P. Soler<sup>60</sup> ,  
 A. Solomin<sup>44,55</sup> , A. Solovev<sup>44</sup> , I. Solovyevev<sup>44</sup> , N. S. Sommerfeld<sup>18</sup> , R. Song<sup>1</sup> ,  
 Y. Song<sup>50</sup> , Y. Song<sup>4,c</sup> , Y. S. Song<sup>6</sup> , F.L. Souza De Almeida<sup>69</sup> , B. Souza De Paula<sup>3</sup> ,  
 E. Spadaro Norella<sup>29,n</sup> , E. Spedicato<sup>25</sup> , J.G. Speer<sup>19</sup> , E. Spiridenkov<sup>44</sup> , P. Spradlin<sup>60</sup> ,  
 V. Sriskaran<sup>49</sup> , F. Stagni<sup>49</sup> , M. Stahl<sup>49</sup> , S. Stahl<sup>49</sup> , S. Stanislaus<sup>64</sup> , E.N. Stein<sup>49</sup> ,  
 O. Steinkamp<sup>51</sup> , O. Stenyakin<sup>44</sup> , H. Stevens<sup>19</sup> , D. Strekalina<sup>44</sup> , Y. Su<sup>7</sup> , F. Suljik<sup>64</sup> ,  
 J. Sun<sup>32</sup> , L. Sun<sup>74</sup> , D. Sundfeld<sup>2</sup> , W. Sutcliffe<sup>51</sup> , P.N. Swallow<sup>54</sup> , K. Swientek<sup>40</sup> ,  
 F. Swystun<sup>56</sup> , A. Szabelski<sup>42</sup> , T. Szumlak<sup>40</sup> , Y. Tan<sup>4,c</sup> , M.D. Tat<sup>64</sup> ,  
 A. Terentev<sup>44</sup> , F. Terzuoli<sup>35,x,49</sup> , F. Teubert<sup>49</sup> , E. Thomas<sup>49</sup> , D.J.D. Thompson<sup>54</sup> ,  
 H. Tilquin<sup>62</sup> , V. Tisserand<sup>11</sup> , S. T'Jampens<sup>10</sup> , M. Tobin<sup>5,49</sup> , L. Tomassetti<sup>26,m</sup> ,  
 G. Tonani<sup>30,o,49</sup> , X. Tong<sup>6</sup> , D. Torres Machado<sup>2</sup> , L. Toscano<sup>19</sup> , D.Y. Tou<sup>4,c</sup> ,

C. Trippel<sup>46</sup> , G. Tuci<sup>22</sup> , N. Tuning<sup>38</sup> , L.H. Uecker<sup>22</sup> , A. Ukleja<sup>40</sup> ,  
D.J. Unverzagt<sup>22</sup> , E. Ursov<sup>44</sup> , A. Usachov<sup>39</sup> , A. Ustyuzhanin<sup>44</sup> , U. Uwer<sup>22</sup> ,  
V. Vagnoni<sup>25,49</sup> , V. Valcarce Cadenas<sup>47</sup> , G. Valenti<sup>25</sup> , N. Valls Canudas<sup>49</sup> ,  
H. Van Hecke<sup>68</sup> , E. van Herwijnen<sup>62</sup> , C.B. Van Hulse<sup>47,z</sup> , R. Van Laak<sup>50</sup> ,  
M. van Veghel<sup>38</sup> , G. Vasquez<sup>51</sup> , R. Vazquez Gomez<sup>45</sup> , P. Vazquez Regueiro<sup>47</sup> ,  
C. Vázquez Sierra<sup>47</sup> , S. Vecchi<sup>26</sup> , J.J. Velthuis<sup>55</sup> , M. Veltri<sup>27,y</sup> , A. Venkateswaran<sup>50</sup> ,  
M. Verdoglia<sup>32</sup> , M. Vesterinen<sup>57</sup> , D. Vico Benet<sup>64</sup> , P. Vidrier Villalba<sup>45</sup> ,  
M. Vieites Diaz<sup>49</sup> , X. Vilasis-Cardona<sup>46</sup> , E. Vilella Figueras<sup>61</sup> , A. Villa<sup>25</sup> ,  
P. Vincent<sup>16</sup> , F.C. Volle<sup>54</sup> , D. vom Bruch<sup>13</sup> , N. Voropaev<sup>44</sup> , K. Vos<sup>79</sup> ,  
G. Vouters<sup>10</sup> , C. Vrahas<sup>59</sup> , J. Wagner<sup>19</sup> , J. Walsh<sup>35</sup> , E.J. Walton<sup>1,57</sup> , G. Wan<sup>6</sup> ,  
C. Wang<sup>22</sup> , G. Wang<sup>8</sup> , H. Wang<sup>73</sup> , J. Wang<sup>6</sup> , J. Wang<sup>5</sup> , J. Wang<sup>4,c</sup> ,  
J. Wang<sup>74</sup> , M. Wang<sup>30</sup> , N. W. Wang<sup>7</sup> , R. Wang<sup>55</sup> , X. Wang<sup>8</sup> , X. Wang<sup>72</sup> , X. W.  
Wang<sup>62</sup> , Y. Wang<sup>6</sup> , Y. H. Wang<sup>73</sup> , Z. Wang<sup>14</sup> , Z. Wang<sup>4,c</sup> , Z. Wang<sup>30</sup> ,  
J.A. Ward<sup>57,1</sup> , M. Waterlaet<sup>49</sup> , N.K. Watson<sup>54</sup> , D. Websdale<sup>62</sup> , Y. Wei<sup>6</sup> ,  
J. Wendel<sup>81</sup> , B.D.C. Westhenry<sup>55</sup> , C. White<sup>56</sup> , M. Whitehead<sup>60</sup> , E. Whiter<sup>54</sup> ,  
A.R. Wiederhold<sup>63</sup> , D. Wiedner<sup>19</sup> , G. Wilkinson<sup>64</sup> , M.K. Wilkinson<sup>66</sup> ,  
M. Williams<sup>65</sup> , M. J. Williams<sup>49</sup> , M.R.J. Williams<sup>59</sup> , R. Williams<sup>56</sup> , Z. Williams<sup>55</sup> ,  
F.F. Wilson<sup>58</sup> , M. Winn<sup>12</sup> , W. Wislicki<sup>42</sup> , M. Witek<sup>41</sup> , L. Witola<sup>22</sup> ,  
G. Wormser<sup>14</sup> , S.A. Wotton<sup>56</sup> , H. Wu<sup>69</sup> , J. Wu<sup>8</sup> , Y. Wu<sup>6</sup> , Z. Wu<sup>7</sup> ,  
K. Wyllie<sup>49</sup> , S. Xian<sup>72</sup> , Z. Xiang<sup>5</sup> , Y. Xie<sup>8</sup> , A. Xu<sup>35</sup> , J. Xu<sup>7</sup> , L. Xu<sup>4,c</sup> ,  
L. Xu<sup>4,c</sup> , M. Xu<sup>57</sup> , Z. Xu<sup>49</sup> , Z. Xu<sup>7</sup> , Z. Xu<sup>5</sup> , D. Yang<sup>4</sup> , K. Yang<sup>62</sup> ,  
S. Yang<sup>7</sup> , X. Yang<sup>6</sup> , Y. Yang<sup>29,n</sup> , Z. Yang<sup>6</sup> , Z. Yang<sup>67</sup> , V. Yeroshenko<sup>14</sup> ,  
H. Yeung<sup>63</sup> , H. Yin<sup>8</sup> , X. Yin<sup>7</sup> , C. Y. Yu<sup>6</sup> , J. Yu<sup>71</sup> , X. Yuan<sup>5</sup> , Y. Yuan<sup>5,7</sup> ,  
E. Zaffaroni<sup>50</sup> , M. Zavertyaev<sup>21</sup> , M. Zdybal<sup>41</sup> , F. Zenesini<sup>25,k</sup> , C. Zeng<sup>5,7</sup> ,  
M. Zeng<sup>4,c</sup> , C. Zhang<sup>6</sup> , D. Zhang<sup>8</sup> , J. Zhang<sup>7</sup> , L. Zhang<sup>4,c</sup> , S. Zhang<sup>64</sup> , S. L.  
Zhang<sup>71</sup> , Y. Zhang<sup>6</sup> , Y. Z. Zhang<sup>4,c</sup> , Y. Zhao<sup>22</sup> , A. Zharkova<sup>44</sup> , A. Zhelezov<sup>22</sup> , S.  
Z. Zheng<sup>6</sup> , X. Z. Zheng<sup>4,c</sup> , Y. Zheng<sup>7</sup> , T. Zhou<sup>6</sup> , X. Zhou<sup>8</sup> , Y. Zhou<sup>7</sup> ,  
V. Zhovkovska<sup>57</sup> , L. Z. Zhu<sup>7</sup> , X. Zhu<sup>4,c</sup> , X. Zhu<sup>8</sup> , V. Zhukov<sup>17</sup> , J. Zhuo<sup>48</sup> ,  
Q. Zou<sup>5,7</sup> , D. Zuliani<sup>33,r</sup> , G. Zunica<sup>50</sup> .

<sup>1</sup>*School of Physics and Astronomy, Monash University, Melbourne, Australia*

<sup>2</sup>*Centro Brasileiro de Pesquisas Físicas (CBPF), Rio de Janeiro, Brazil*

<sup>3</sup>*Universidade Federal do Rio de Janeiro (UFRJ), Rio de Janeiro, Brazil*

<sup>4</sup>*Department of Engineering Physics, Tsinghua University, Beijing, China*

<sup>5</sup>*Institute Of High Energy Physics (IHEP), Beijing, China*

<sup>6</sup>*School of Physics State Key Laboratory of Nuclear Physics and Technology, Peking University, Beijing, China*

<sup>7</sup>*University of Chinese Academy of Sciences, Beijing, China*

<sup>8</sup>*Institute of Particle Physics, Central China Normal University, Wuhan, Hubei, China*

<sup>9</sup>*Consejo Nacional de Rectores (CONARE), San Jose, Costa Rica*

<sup>10</sup>*Université Savoie Mont Blanc, CNRS, IN2P3-LAPP, Annecy, France*

<sup>11</sup>*Université Clermont Auvergne, CNRS/IN2P3, LPC, Clermont-Ferrand, France*

<sup>12</sup>*Université Paris-Saclay, Centre d'Etudes de Saclay (CEA), IRFU, Gif-Sur-Yvette, France*

<sup>13</sup>*Aix Marseille Univ, CNRS/IN2P3, CPPM, Marseille, France*

<sup>14</sup>*Université Paris-Saclay, CNRS/IN2P3, IJCLab, Orsay, France*

<sup>15</sup>*Laboratoire Leprince-Ringuet, CNRS/IN2P3, Ecole Polytechnique, Institut Polytechnique de Paris, Palaiseau, France*

<sup>16</sup>*Laboratoire de Physique Nucléaire et de Hautes Énergies (LPNHE), Sorbonne Université, CNRS/IN2P3, Paris, France*

<sup>17</sup>*I. Physikalisches Institut, RWTH Aachen University, Aachen, Germany*

<sup>18</sup>*Universität Bonn - Helmholtz-Institut für Strahlen und Kernphysik, Bonn, Germany*

<sup>19</sup>*Fakultät Physik, Technische Universität Dortmund, Dortmund, Germany*

<sup>20</sup>*Physikalisches Institut, Albert-Ludwigs-Universität Freiburg, Freiburg, Germany*

- <sup>21</sup> *Max-Planck-Institut für Kernphysik (MPIK), Heidelberg, Germany*
- <sup>22</sup> *Physikalisches Institut, Ruprecht-Karls-Universität Heidelberg, Heidelberg, Germany*
- <sup>23</sup> *School of Physics, University College Dublin, Dublin, Ireland*
- <sup>24</sup> *INFN Sezione di Bari, Bari, Italy*
- <sup>25</sup> *INFN Sezione di Bologna, Bologna, Italy*
- <sup>26</sup> *INFN Sezione di Ferrara, Ferrara, Italy*
- <sup>27</sup> *INFN Sezione di Firenze, Firenze, Italy*
- <sup>28</sup> *INFN Laboratori Nazionali di Frascati, Frascati, Italy*
- <sup>29</sup> *INFN Sezione di Genova, Genova, Italy*
- <sup>30</sup> *INFN Sezione di Milano, Milano, Italy*
- <sup>31</sup> *INFN Sezione di Milano-Bicocca, Milano, Italy*
- <sup>32</sup> *INFN Sezione di Cagliari, Monserrato, Italy*
- <sup>33</sup> *INFN Sezione di Padova, Padova, Italy*
- <sup>34</sup> *INFN Sezione di Perugia, Perugia, Italy*
- <sup>35</sup> *INFN Sezione di Pisa, Pisa, Italy*
- <sup>36</sup> *INFN Sezione di Roma La Sapienza, Roma, Italy*
- <sup>37</sup> *INFN Sezione di Roma Tor Vergata, Roma, Italy*
- <sup>38</sup> *Nikhef National Institute for Subatomic Physics, Amsterdam, Netherlands*
- <sup>39</sup> *Nikhef National Institute for Subatomic Physics and VU University Amsterdam, Amsterdam, Netherlands*
- <sup>40</sup> *AGH - University of Krakow, Faculty of Physics and Applied Computer Science, Kraków, Poland*
- <sup>41</sup> *Henryk Niewodniczanski Institute of Nuclear Physics Polish Academy of Sciences, Kraków, Poland*
- <sup>42</sup> *National Center for Nuclear Research (NCBJ), Warsaw, Poland*
- <sup>43</sup> *Horia Hulubei National Institute of Physics and Nuclear Engineering, Bucharest-Magurele, Romania*
- <sup>44</sup> *Authors affiliated with an institute formerly covered by a cooperation agreement with CERN.*
- <sup>45</sup> *ICCUB, Universitat de Barcelona, Barcelona, Spain*
- <sup>46</sup> *La Salle, Universitat Ramon Llull, Barcelona, Spain*
- <sup>47</sup> *Instituto Galego de Física de Altas Enerxías (IGFAE), Universidade de Santiago de Compostela, Santiago de Compostela, Spain*
- <sup>48</sup> *Instituto de Física Corpuscular, Centro Mixto Universidad de Valencia - CSIC, Valencia, Spain*
- <sup>49</sup> *European Organization for Nuclear Research (CERN), Geneva, Switzerland*
- <sup>50</sup> *Institute of Physics, Ecole Polytechnique Fédérale de Lausanne (EPFL), Lausanne, Switzerland*
- <sup>51</sup> *Physik-Institut, Universität Zürich, Zürich, Switzerland*
- <sup>52</sup> *NSC Kharkiv Institute of Physics and Technology (NSC KIPT), Kharkiv, Ukraine*
- <sup>53</sup> *Institute for Nuclear Research of the National Academy of Sciences (KINR), Kyiv, Ukraine*
- <sup>54</sup> *School of Physics and Astronomy, University of Birmingham, Birmingham, United Kingdom*
- <sup>55</sup> *H.H. Wills Physics Laboratory, University of Bristol, Bristol, United Kingdom*
- <sup>56</sup> *Cavendish Laboratory, University of Cambridge, Cambridge, United Kingdom*
- <sup>57</sup> *Department of Physics, University of Warwick, Coventry, United Kingdom*
- <sup>58</sup> *STFC Rutherford Appleton Laboratory, Didcot, United Kingdom*
- <sup>59</sup> *School of Physics and Astronomy, University of Edinburgh, Edinburgh, United Kingdom*
- <sup>60</sup> *School of Physics and Astronomy, University of Glasgow, Glasgow, United Kingdom*
- <sup>61</sup> *Oliver Lodge Laboratory, University of Liverpool, Liverpool, United Kingdom*
- <sup>62</sup> *Imperial College London, London, United Kingdom*
- <sup>63</sup> *Department of Physics and Astronomy, University of Manchester, Manchester, United Kingdom*
- <sup>64</sup> *Department of Physics, University of Oxford, Oxford, United Kingdom*
- <sup>65</sup> *Massachusetts Institute of Technology, Cambridge, MA, United States*
- <sup>66</sup> *University of Cincinnati, Cincinnati, OH, United States*
- <sup>67</sup> *University of Maryland, College Park, MD, United States*
- <sup>68</sup> *Los Alamos National Laboratory (LANL), Los Alamos, NM, United States*
- <sup>69</sup> *Syracuse University, Syracuse, NY, United States*
- <sup>70</sup> *Pontifícia Universidade Católica do Rio de Janeiro (PUC-Rio), Rio de Janeiro, Brazil, associated to <sup>3</sup>*
- <sup>71</sup> *School of Physics and Electronics, Hunan University, Changsha City, China, associated to <sup>8</sup>*
- <sup>72</sup> *State Key Laboratory of Nuclear Physics and Technology, South China Normal University, Guangzhou, China, associated to <sup>4</sup>*
- <sup>73</sup> *Lanzhou University, Lanzhou, China, associated to <sup>5</sup>*

- <sup>74</sup> *School of Physics and Technology, Wuhan University, Wuhan, China, associated to* <sup>4</sup>  
<sup>75</sup> *Departamento de Física , Universidad Nacional de Colombia, Bogota, Colombia, associated to* <sup>16</sup>  
<sup>76</sup> *Ruhr Universitaet Bochum, Fakultaet f. Physik und Astronomie, Bochum, Germany, associated to* <sup>19</sup>  
<sup>77</sup> *Eotvos Lorand University, Budapest, Hungary, associated to* <sup>49</sup>  
<sup>78</sup> *Van Swinderen Institute, University of Groningen, Groningen, Netherlands, associated to* <sup>38</sup>  
<sup>79</sup> *Universiteit Maastricht, Maastricht, Netherlands, associated to* <sup>38</sup>  
<sup>80</sup> *Tadeusz Kosciuszko Cracow University of Technology, Cracow, Poland, associated to* <sup>41</sup>  
<sup>81</sup> *Universidade da Coruña, A Coruña, Spain, associated to* <sup>46</sup>  
<sup>82</sup> *Department of Physics and Astronomy, Uppsala University, Uppsala, Sweden, associated to* <sup>60</sup>  
<sup>83</sup> *University of Michigan, Ann Arbor, MI, United States, associated to* <sup>69</sup>

- <sup>a</sup> *Universidade Estadual de Campinas (UNICAMP), Campinas, Brazil*  
<sup>b</sup> *Centro Federal de Educação Tecnológica Celso Suckow da Fonseca, Rio De Janeiro, Brazil*  
<sup>c</sup> *Center for High Energy Physics, Tsinghua University, Beijing, China*  
<sup>d</sup> *Hangzhou Institute for Advanced Study, UCAS, Hangzhou, China*  
<sup>e</sup> *School of Physics and Electronics, Henan University , Kaifeng, China*  
<sup>f</sup> *LIP6, Sorbonne Université, Paris, France*  
<sup>g</sup> *Lamarr Institute for Machine Learning and Artificial Intelligence, Dortmund, Germany*  
<sup>h</sup> *Universidad Nacional Autónoma de Honduras, Tegucigalpa, Honduras*  
<sup>i</sup> *Università di Bari, Bari, Italy*  
<sup>j</sup> *Università di Bergamo, Bergamo, Italy*  
<sup>k</sup> *Università di Bologna, Bologna, Italy*  
<sup>l</sup> *Università di Cagliari, Cagliari, Italy*  
<sup>m</sup> *Università di Ferrara, Ferrara, Italy*  
<sup>n</sup> *Università di Genova, Genova, Italy*  
<sup>o</sup> *Università degli Studi di Milano, Milano, Italy*  
<sup>p</sup> *Università degli Studi di Milano-Bicocca, Milano, Italy*  
<sup>q</sup> *Università di Modena e Reggio Emilia, Modena, Italy*  
<sup>r</sup> *Università di Padova, Padova, Italy*  
<sup>s</sup> *Università di Perugia, Perugia, Italy*  
<sup>t</sup> *Scuola Normale Superiore, Pisa, Italy*  
<sup>u</sup> *Università di Pisa, Pisa, Italy*  
<sup>v</sup> *Università della Basilicata, Potenza, Italy*  
<sup>w</sup> *Università di Roma Tor Vergata, Roma, Italy*  
<sup>x</sup> *Università di Siena, Siena, Italy*  
<sup>y</sup> *Università di Urbino, Urbino, Italy*  
<sup>z</sup> *Universidad de Alcalá, Alcalá de Henares , Spain*  
<sup>aa</sup> *Department of Physics/Division of Particle Physics, Lund, Sweden*

† *Deceased*